THE EFFECT OF TEMPERATURE ON DRAWABILITY OF CIRCULAR AND SQUARE SHEET METAL DRAWING

MUHAMMAD BASRIL BIN MUHAMMAD ASRI

FACULTY OF ENGINEERING
UNIVERSITY OF MALAYA
KUALA LUMPUR

2022

THE EFFECT OF TEMPERATURE ON DRAWABILITY OF CIRCULAR AND SQUARE SHEET METAL DRAWING

MUHAMMAD BASRIL BIN MUHAMMAD ASRI

THESIS SUBMITTED IN FULFILMENT OF THE REQUIREMENTS FOR THE DEGREE OF MASTER OF ENGINEERING SCIENCE

FACULTY OF ENGINEERING
UNIVERSITY OF MALAYA
KUALA LUMPUR

2022

UNIVERSITY OF MALAYA

ORIGINAL LITERARY WORK DECLARATION

Name of Candidate: MUHAMMAD BASRIL BIN MUHAMMAD ASRI

I.C/Passport No:

Matric No: KGA150063/17050398

Name of Degree: MASTER OF ENGINEERING SCIENCE

Title of Project Paper/Research Report/Dissertation/Thesis ("this Work"):

THE EFFECT OF TEMPERATURE ON DRAWABILITY OF CIRCULAR AND SQUARE SHEET METAL DRAWING

Field of Study:

MANUFACTURING PROCESS (ENGINEERING AND ENGINEERING TRADES)

I do solemnly and sincerely declare that:

(1) I am the sole author/writer of this Work;
(2) This Work is original;
(3) Any use of any work in which copyright exists was done by way of fair dealing and for permitted purposes and any excerpt or extract from, or reference to or reproduction of any copyright work has been disclosed expressly and sufficiently and the title of the Work and its authorship have been acknowledged in this Work;
(4) I do not have any actual knowledge nor do I ought reasonably to know that the making of this work constitutes an infringement of any copyright work;
(5) I hereby assign all and every rights in the copyright to this Work to the University of Malaya ("UM"), who henceforth shall be owner of the copyright in this Work and that any reproduction or use in any form or by any means whatsoever is prohibited without the written consent of UM having been first had and obtained;
(6) I am fully aware that if in the course of making this Work I have infringed any copyright whether intentionally or otherwise, I may be subject to legal action or any other action as may be determined by UM.

Candidate's Signature: Date:

Subscribed and solemnly declared before,

Witness's Signature: Date:

Name: DR AZUDDIN MAMAT

Designation: SENIOR LECTURER

UNIVERSITI MALAYA

PERAKUAN KEASLIAN PENULISAN

Nama: MUHAMMAD BASRIL BIN MUHAMMAD ASRI

No. K.P/Pasport:

No. Matrik: KGA150063/17050398

Nama Ijazah: SARJANA SAINS KEJURUTER AAN

Tajuk Kertas Projek/Laporan Penyelidikan/Disertasi/Tesis ("Hasil Kerja ini"):

KESAN SUHU TERHADAP KEBOLEHBENTUKAN PEMBENTUKAN LEMBARAN CAWAN BULAT DAN PERSEGI

Bidang Penyelidikan: PROSES PEMBUATAN

Saya dengan sesungguhnya dan sebenarnya mengaku bahawa:

(1) Saya adalah satu-satunya pengarang/penulis Hasil Kerja ini;
(2) Hasil Kerja ini adalah asli;
(3) Apa-apa penggunaan mana-mana hasil kerja yang mengandungi hakcipta telah dilakukan secara urusan yang wajar dan bagi maksud yang dibenarkan dan apa-apa petikan, ekstrak, rujukan atau pengeluaran semula daripada atau kepada mana-mana hasil kerja yang mengandungi hakcipta telah dinyatakan dengan sejelasnya dan secukupnya dan satu pengiktirafan tajuk hasil kerja tersebut dan pengarang/penulisnya telah dilakukan di dalam Hasil Kerja ini;
(4) Saya tidak mempunyai apa-apa pengetahuan sebenar atau patut semunasabahnya tahu bahawa penghasilan Hasil Kerja ini melanggar suatu hakcipta hasil kerja yang lain;
(5) Saya dengan ini menyerahkan kesemua dan tiap-tiap hak yang terkandung di dalam hakcipta Hasil Kerja ini kepada Universiti Malaya ("UM") yang seterusnya mula dari sekarang adalah tuan punya kepada hakcipta di dalam Hasil Kerja ini dan apa-apa pengeluaran semula atau penggunaan dalam apa jua bentuk atau dengan apa juga cara sekalipun adalah dilarang tanpa terlebih dahulu mendapat kebenaran bertulis dari UM;
(6) Saya sedar sepenuhnya sekiranya dalam masa penghasilan Hasil Kerja ini saya telah melanggar suatu hakcipta hasil kerja yang lain sama ada dengan niat atau sebaliknya, saya boleh dikenakan tindakan undang-undang atau apa-apa tindakan lain sebagaimana yang diputuskan oleh UM.

Tandatangan Calon: Tarikh:

Diperbuat dan sesungguhnya diakui di hadapan,

Tandatangan Saksi: Tarikh:

Nama: DR AZUDDIN MAMAT

Jawatan: PENSYARAH KANAN

ABSTRACT

Sheet metal drawing is a well-known process used in today's industries, and the most significant challenge encountered throughout this process is product quality. In sheet metal drawing, product quality is vital and based on current research trends, varying the process temperature improves the quality.

This study focuses on the influence of tooling temperature on the drawability of sheet metal drawn circular and square cups with various blank sizes. Following that, an evaluation of the impact of different process parameters on the warm sheet metal drawing was carried out. Consequently, the drawability of circular and square cups will be analysed by comparing experimental and finite element analysis (FEA) data.

The Taguchi method L9 (3^4) array experiment design was used to plan the process parameters and the experimental design in this study. The experimental procedures were prepared with the experimental apparatus's consideration. The experimental setup apparatus for circular and square cups, which includes a die set, heater, thermocouple, hydraulic pump and cylinder, is then put through a series of tests. Firstly, circular cups of aluminium 6065 (AL6065), mild steel (MS), and stainless steel 304 (SS304) were drawn from the blank with diameters of 60 mm, 65 mm, and 70 mm. Next, the same material was drawn for square cups with a blank diameter of 45 mm, 50 mm, and 55 mm. Both cup shape is tested at room temperature, then at temperatures of 100°C, 150°C, and 200°C.

The response factors consist of limiting drawing ratio (LDR), average cup height and thickness distribution were collected from room and warm temperatures. First, these outputs were analysed using the analysis of variance (ANOVA) to determine their effect on warm sheet metal drawing. Then, the sheet metal drawing process is simulated using ABAQUS/CAE software to predict the drawn cup thickness distribution. Eventually, the simulated data will be compared with the experiment for verification.

From the ANOVA analysis, the blank material had the most significant impact on the drawability of warm sheet metal drawn circular cups, followed by the blank size, heating technique, and heating temperature. The optimal parameter was 65 mm of the AL6065 blank with a heating temperature of 150°C applied to the punch. On the other hand, the drawability of warm sheet metal drawn square cups was substantially impacted by the blank size, followed by the material, heating technique, and heating temperature. The optimal parameter was 45 mm of the AL6065 blank with a heating temperature of 150°C applied to the punch.

Keywords: Sheet metal drawing; Taguchi Method; Circular and square cup.

ABSTRAK

Penarikan kepingan logam ialah proses terkenal yang digunakan dalam industri hari ini, dan cabaran paling ketara yang dihadapi sepanjang proses ini ialah kualiti produk. Dalam penarikan dalam, kualiti produk adalah penting dan berdasarkan penyelidikan semasa, perubahan suhu proses dapat meningkatkan kualiti.

Kajian ini memberi tumpuan kepada pengaruh suhu set acuan terhadap kebolehbentukan cawan bulat dan persegi pelbagai saiz. Sehubungan itu, penilaian kesan pelbagai parameter proses yang berbeza pada penarikan kepingan logam hangat telah dijalankan. Justeru itu, kebolehbentukan cawan bulat dan persegi akan dinilai dengan membandingkan data eksperimen dan analisis unsur terhingga (FEA).

Dalam kajian ini, tatasusunan L9 (3^4) kaedah Taguchi digunakan bagi merancang parameter proses dan reka bentuk eksperimen. Selepas itu, prosedur eksperimen telah disediakan dengan mengambil kira peranti eksperimen. Peranti eksperimen yang terlibat dalam proses penarikan cawan bulat dan persegi ialah set acuan, pemanas, termokopel, pam dan silinder hidraulik yang kemudian akan menjalani satu siri ujian. Pertama, proses penarikan cawan logam bulatan aluminium 6065 (AL6065), keluli lembut (MS), dan keluli tahan karat 304 (SS304) telah dijalankan dengan menggunakan kepingan logam yang berdiameter 60 mm, 65 mm, dan 70 mm. Manakala, bagi proses penarikan cawan logam persegi pula, ia menggunakan bahan kepingan logam yang sama dengan saiz 45 mm, 50 mm, dan 55 mm. Kedua-dua bentuk cawan menjalani eksperimen pada suhu bilik dan kemudian pada 100°C, 150°C dan 200°C.

Keputusan eksperimen terdiri daripada nisbah had penarikan (LDR), purata ketinggian cawan, dan agihan ketebalan sepanjang profil cawan diambil daripada eksperimen yang dijalankan di suhu bilik dan suhu panas. Keputusan ini dianalisis menggunakan pendekatan statistik varians (ANOVA) bagi menentukan kesannya terhadap proses penarikan kepingam logam hangat. Kemudian, proses penarikan akan disimulasikan

dalam perisian ABAQUS/CAE meramalkan agihan ketebalan dinding cawan. Seterusnya, data simulasi akan dibandingkan dengan eksperimen bagi tujuan verifikasi.

Daripada analisis ANOVA, bahan kepingan logam mempunyai kesan yang paling ketara terhadap kebolehbentukan cawan bulat yang dihasilkan daripada suhu panas, diikuti dengan saiz kepingan logam, teknik pemanasan dan suhu pemanasan. Parameter yang paling optimum bagi proses penarikan dalam cawan bulat ialah kepingan 65 mm AL6065 dengan aplikasi suhu pemanasan 150°C pada penebuk. Sebaliknya, bagi kebolehbentukan cawan persegi yang dihasilkan pada suhu panas paling dipengaruhi oleh saiz kepingan logam, diikuti oleh bahan kepingan logam, teknik dan suhu pemanasan. Parameter optimum bagi proses penarikan dalam cawan persegi ialah kepingan 45 mm AL6065 dengan aplikasi suhu pemanasan 150°C pada penebuk.

Kata kunci: Proses penarikan kepingan logam; Kaedah Taguchi; Cawan logam bulatan; Cawan logam persegi.

ACKNOWLEDGEMENTS

First and foremost, praise and thanks to Allah the Almighty for His showers of blessings throughout my research work to complete this research successfully. I want to express my deep and sincere gratitude to my research supervisors, Dr. Azuddin Mamat and Professor Dr. Imtiaz Ahmed Choudhury, for the opportunity, continuous guidance, advice, invaluable assistance, and encouragement throughout this research. I also really appreciate their willingness to share their expertise in this field of study, which has significantly aided the completion of this research. Their vision and sincerity in guiding me in technical and writing knowledge have profoundly motivated and inspired me.

I would also like to thank the Mechanical Engineering Department supporting staff for their assistance throughout my studies. The invaluable experience shared from them, especially during the experimental design setup, really broadened my horizon in terms of technical knowledge application. Besides that, I would like to thank my fellow postgraduate colleagues who gave me continuous support and motivation throughout my studies.

Lastly, I am incredibly grateful to my mother, Betmawati binti Jaunis, for her love, prayers, and sacrifices to educate me and prepare me for my future. I am also very thankful to my sisters, Nur Rashidah and Nur Izettie, for their support and understanding of my passion and interest. Not to forget, Raja Putri Naquiah for her kind support and attention towards me during the completion of this work. I dedicate this thesis to them as a token of appreciation for believing in me all these years.

TABLE OF CONTENTS

Abstract iii

Abstrak v

Acknowledgements 7

Table of Contents 8

List of Figures 11

List of Tables 13

List of Symbols and Abbreviations 15

List of Appendices 17

CHAPTER 1: INTRODUCTION 18

1.1 Background 18

1.2 Research objectives 19

1.3 Scope of research 19

1.4 Research outline 20

CHAPTER 2: LITERATURE REVIEW 21

2.1 Introduction 21

2.2 Deep drawing 22

2.3 Warm deep drawing 24

2.4 The shape of the sheet metal drawn cup 25

2.5 Limiting drawing ratio (LDR) 26

2.6 Drawability 27

2.6.1 Tools of the sheet metal drawing process 29

2.6.2 Punching speed 30

2.6.3 Thickness distribution 30

2.7 Materials 31

2.7.1 Aluminium 31

2.7.2 Mild steel (Low carbon steel) 32
2.7.3 Stainless steel 32
2.8 Design of experiment and quality characteristic analysis 33
2.8.1 Taguchi method 34
2.8.2 Signal-to-noise ratio analysis 34
2.8.3 Analysis of Variance (ANOVA) 35
2.9 Defects in the sheet metal drawing process 36
2.10 Finite element analysis (FEA) 37
2.11 Summary of literatures 38
CHAPTER 3: RESEARCH METHODOLOGY 39
3.1 Research Methodology 39
3.1.1 Experimental setup 41
3.1.2 Die set for circular cup 43
3.1.3 Die set for square cup 45
3.1.4 Material selection 45
3.1.5 Design of experiment using Taguchi approach 46
3.1.6 Experiment's parameters 47
3.1.7 Orthogonal array 48
3.1.8 Procedures 50
3.2 Data collection and analysis 51
3.2.1 Quality measurement methods 51
3.2.2 Analysis of variance (ANOVA) 52
3.2.3 Finite element analysis (FEA) 53
CHAPTER 4: RESULTS AND DISCUSSION 56
4.1 Introduction 56
4.2 Circular sheet metal drawn cup 56

4.2.1 Limiting drawing ratio (LDR) for the circular cup 56
4.2.2 Average circular sheet metal drawn cup height 58
4.2.3 Thickness distribution of the circular cup 59
4.2.4 Simulation 64
4.2.5 S/N Ratio and ANOVA for the circular cup 67
4.2.6 Confirmation test for circular cup 70
4.3 Square sheet metal drawn cup 71
4.3.1 Limiting drawing ratio (LDR) for the square cup 71
4.3.2 Average square cup height 72
4.3.3 Thickness distribution for the square cup 74
4.3.4 Simulation 80
4.3.5 S/N Ratio and ANOVA for the square cup 82
4.3.6 Confirmation test for square cup 85
CHAPTER 5: CONCLUSION 86
5.1 Introduction 86
5.2 Conclusion 86
5.2.1 The effect of tooling temperature on circular and square sheet metal drawing 86
5.2.2 The effect of different process parameters on warm sheet metal drawing 87
5.2.3 Comparison of the thickness distribution within the drawn cup between experiment and finite element analysis 88
5.3 Recommendations 89
References 90
Publications 135

LIST OF FIGURES

Figure 2.1: Workpiece stresses during deep drawing (Colgan & Monaghan, 2003) 23

Figure 2.2: Deformation and necking of workpiece (Colgan & Monaghan, 2003) 23

Figure 3.1: Research Design 40

Figure 3.2: Experimental setup for warm and room temperature sheet metal drawing .. 41

Figure 3.3: Circular die set 44

Figure 3.4: Square die set 45

Figure 3.5: Blank samples with different sizes for circular and square sheet metal drawing 50

Figure 4.1: Average sheet metal drawn circular cup's height for AL6065, MS, and stainless versus blank diameter 58

Figure 4.2: Illustration of measuring position along the circular cup's profile 59

Figure 4.3: Thickness distribution along the circular cup profile in the sheet metal drawing process conducted at (a) room temperature and (b) warm temperature 60

Figure 4.4: 3D model of circular sheet metal drawing tools setup 65

Figure 4.5: FEA on thickness distribution for the circular sheet metal drawing process 65

Figure 4.6: Main effect plot for S/N ratio of thickness distribution for the circular cup 68

Figure 4.7: 65 mm AL6065 circular cup drawn at 150°C heated punch 70

Figure 4.8: Thickness distribution of 65 mm AL6065 circular cup drawn at 150°C heated punch 70

Figure 4.9: Average square sheet metal drawn cup's height for AL6065, MS, and SS304 versus blank diameter 73

Figure 4.10: Illustration of measuring position along the square cup profile 74

Figure 4.11: Thickness distribution along the square cup profile in the sheet metal drawing process conducted at (a) room temperature and (b) warm temperature 75

Figure 4.12: 3D model of square sheet metal drawing tool setup 80

Figure 4.13: FEA on thickness distribution for circular sheet metal drawing process ... 80

Figure 4.14: Main effect plot for S/N ratio of thickness distribution for the square cup 83

Figure 4.15: 45 mm AL6065 circular cup drawn at 150°C heated punch 85

Figure 4.8: Thickness distribution of 45 mm AL6065 circular cup drawn at 150°C heated punch 85

LIST OF TABLES

Table 3.1: Specification of hydraulic cylinder *(source: http://www.enerpac.com)* 41

Table 3.2: Specification for force sensor with the data acquisition system 43

Table 3.3: Tooling dimension for circular blank 44

Table 3.4: Tooling dimension for square blank 45

Table 3.5: Mechanical and thermal properties of aluminium 6065, MS, and SS304 (Groover, 2013) 46

Table 3.6: Selected factors and levels for circular sheet metal drawing 48

Table 3.7: Selected factors and levels for square sheet metal drawing 48

Table 3.8: L9 Orthogonal array 48

Table 3.9: L9 Orthogonal array for circular and square sheet metal drawing in warm condition 49

Table 3.10: Experiments for circular and square sheet metal drawing at room temperature 49

Table 3.11: Quality measurement methods 51

Table 4.1: LDR for circular cups of AL6065, MS and SS304 in the room and warm sheet metal drawing 57

Table 4.2: Analysis of thickness distribution in circular sheet metal drawing experiment 62

Table 4.3: Analysis of thickness distribution in circular sheet metal drawing simulation from ABAQUS 66

Table 4.4: Response table for S/N ratio of thickness distribution for the circular cup ... 68

Table 4.5: Optimal condition for warm sheet metal drawing of the circular cup to achieve good thickness distribution 69

Table 4.6: Contribution of process parameters on warm sheet metal drawing process to achieve good thickness distribution of the circular cup 69

Table 4.7: LDR for AL6065, MS, and SS304 in the room and warm sheet metal drawing for the square cup 71

Table 4.8: Analysis of thickness distribution in square sheet metal drawing experiment 77

Table 4.9: Analysis of thickness distribution in square sheet metal drawing simulation from ABAQUS 81

Table 4.10: Response table for S/N ratio of thickness distribution for the square cup ... 83

Table 4.11: Optimal condition for warm sheet metal drawing of the square cup to achieve good thickness distribution 84

Table 4.12: Contribution of process parameters on warm sheet metal drawing process to achieve good thickness distribution of the square cup 84

LIST OF SYMBOLS AND ABBREVIATIONS

r_2	:	Die corner radius
t_0	:	Initial blank thickness
c/t_0	:	Die clearance
AL6065	:	Aluminium 6065
MS	:	Mild steel
SS304	:	Stainless steel 304
LDR	:	Limiting drawing ratio
BHP	:	Blank holding pressure
FEA	:	Finite element analysis
ANOVA	:	Analysis of variance
S/N ratio	:	Signal to noise ratio
$\frac{D}{d}$	:	Drawing ratio
$\frac{t}{D}$	:	Thickness ratio
F_p	:	Punch force
σ_y	:	Yield stress
η	:	Deformation efficiency factor
P_y	:	Initial yielding load
P_{max}	:	Maximum load
r_M	:	Die edge curvature
D	:	Diameter of the blank
d	:	Diameter of punch
s	:	Sheet thickness
VBHF	:	Variable blank holder force

F_{dr}	:	Drawing force
C	:	Circumference of the drawing punch
R_M	:	Tensile strength
n	:	Correction value
vM	:	Von Mises criterion
FLD	:	Forming limit diagram
T	:	Mean of total S/N ratio for optimum factor
i	:	Counter
n	:	Total number of experiment trials
$\frac{\bar{S}}{N}$	:	Overall mean S/N ratio
SS_T	:	Sum of square deviation
SS_y	:	Sum of square deviation
ρ	:	Percentage distributions
RT	:	Room temperature
BHF	:	Blank holding force
3D	:	Three-dimensional
2D	:	Two-dimensional
BC	:	Boundary condition

LIST OF APPENDICES

Appendix A…… 95

Appendix B…… 97

Appendix C…… 107

Appendix D…… 117

Appendix E…… 119

Appendix F…… 127

CHAPTER 1: INTRODUCTION

1.1 Background

Nowadays, manufacturers compete fiercely to stay relevant in the market, driven by the rapid growth of manufacturing technological improvement. Manufacturers frequently enhance production performance without compromising product quality by reducing manufacturing costs. Typically, manufacturing costs comprise materials, labour, and overhead. However, when production increases, manufacturing costs increase.

Sheet metal drawing is a prominent manufacturing process, especially for making automobiles and household appliances. Recent studies show that process temperature impacts drawability and that sheet metal drawing improvement is achievable under certain conditions. Current studies focus on warm sheet metal drawings of aluminium and magnesium alloys.

Warm stamped parts are the latest trend among automakers globally to produce stronger and lighter chassis. For example, safety components such as A-pillars, side-impact bars, and roof rails were manufactured using a warm sheet metal drawing process involving heating the steel blank to an austenitization temperature. The heated blank enters the tool, which simultaneously shapes and quenches the blank to strengthen it.

The goals of the manufacturing process improvement were not only cost reduction but also maintaining product quality and leading to customer satisfaction. Finite element analysis (FEA) is a powerful tool for simulating forming processes and accurately forecasting deformation behaviours. FEA can estimate the optimum conditions of forming processes in analysis and design. Incorporating FEA in warm sheet metal drawing allows the manufacturer to control process parameters and minimize severe defects.

1.2 Research objectives

The objectives of this research are:

1. To investigate the tooling temperature effect on improvement of wall thickness distribution for circular and square sheet metal drawn cups.
2. To evaluate and optimize the effect of blank material, blank size, heating temperature and heating technique towards warm circular and square sheet metal drawing using Taguchi method.
3. To compare the drawability of circular and square sheet metal drawn cups experimentally and by finite element analysis (FEA) result.

1.3 Scope of research

The temperature gradient can improve the sheet metal drawing process. Thus, this study examines how the application of warm temperature to the sheet metal drawing process improves the drawability of circular and square cups.

This study compares the drawability of circular and square sheet metal drawn cups at room and warm temperatures. The materials involved were Aluminium 6065 (AL6065), Mild Steel (MS), and Stainless Steel 304 (SS304). The drawability consists of limiting drawing ratio (LDR), average cup height, and thickness distribution along the cup profile. For the warm temperature, it will range from 100°C to 200°C. The design of experiment will utilize Taguchi method, and experimental data will be statistically analysed using the S/N ratio and ANOVA. Additionally, the cup's wall thickness distribution from the experiment will be compared to the FEA results generated by ABAQUS software in three-dimensional (3D) visual graphs.

1.4 Research outline

The dissertation is divided into five chapters. The chapters describe the content as follows:

Chapter 1 provides context for the sheet metal drawing technique and the underlying issue before outlining the objectives, scope, and restrictions.

Chapter 2 contains a brief explanation of the review of pertinent literature. The literature review focuses on the sheet metal drawing process, thermal gradient application, quality characteristics, defects, and FEA.

Chapter 3 highlights the research methodology. It describes the experimental materials and apparatus, the experimental design, the procedures, the statistical and FEA analysis.

Chapter 4 describes the outcome of the experimental investigation for circular and square cups, quality characteristics analysis (LDR, average cup's height, and thickness distribution), and comparison of thickness distribution obtained from FEA and experiment.

Chapter 5 outlines the findings and significant contributions to the research field. This chapter also mentions a recommendation for future work to achieve better cup wall thickness distribution through the warm sheet metal drawing process.

CHAPTER 2: LITERATURE REVIEW

2.1 Introduction

The sheet metal drawing was a sheet forming process used in many industries. Ambrogio et al. (2005) state that deep drawing is utilized in manufacturing household utilities, automotive, and aviation components. Several studies were conducted to reduce manufacturing costs by manipulating the workpiece's plastic deformation mechanics in the deep drawing process (El-Morsy & Manabe, 2006). One of the methods was applying thermal gradient towards the deep drawing process, which could influence drawability under appropriate conditions (Takuda et al., 2003).

Diverse sheet metal materials were employed in the deep drawing process for various industries. For example, Moon et al. (2001) conducted tool temperature control research using stainless steel's blank, while Ghaffari Tari et al. (2013) conducted an experimental study for deep drawing of AZ31B magnesium alloy. On the other hand, Nguyen et al. (2014) studied the process parameters optimization of deep drawing using aluminium 6061 sheets.

Different shapes of deep-drawn cups will have various dimensional defects, which cause a significant challenge for industries that mass produce their products. One way to minimize the defect is using simulation or FEA to forecast the outcome before applying it to the manufacturing line. FEA will analyse the deformation behaviour seen through the tests and introduced in simulation (Takuda et al., 2003). FEA also allows the user to evaluate multiple process parameter combinations to obtain the optimum result. Hence, the manufacturer can assess the impact of process improvement on productivity by comparing FEA and experimental data output.

2.2 Deep drawing

Deep drawing is a mechanical process that turns flat sheet metal into three-dimensional (3D) objects. The transformation can create either in a single step or in a sequence of operations (Suchy, 2006). According to Tschaetsch (2004), deep drawing shapes the sheet metals into cup shapes by tension and compressive forces. The process utilizes a blank holder, drawing die and punch. This procedure must fulfil no failure criteria and excessive localised thinning (Gavas & Izciler, 2007).

Referring to Bong et al. (2013), deep drawing is among the most generally applied tests used to analyse the drawability of sheet metals. The cup will undergo a step process involving a blank and die-punch set. The blank will be positioned on top of the die and firmly held in place by the blank holder to minimise defects. Next, the punch presses the blank with a certain speed and pressure based on setup specifications.

According to Colgan and Monaghan (2003), the blank is subjected to three types of stress during the process. Radial stress will be at the flange area (A) as the blank pulls towards the die cavity. Additionally, blank holder pressure applies normal compressive stress to the element. The radial tensile stresses lead to compressive hoop stresses as the reductions in circumferential direction take place. The blank's flange attempts to wrinkle as this hoop stress is applied, but the blank holder will prevent it. On the other hand, at element (B), the cup's wall primarily experiences longitudinal tensile stress. The punch transmits the drawing force through the wall of the cup and the flange as it draws towards the die cavity direction. The element (A) and (B) can be observed in Figure 2.1.

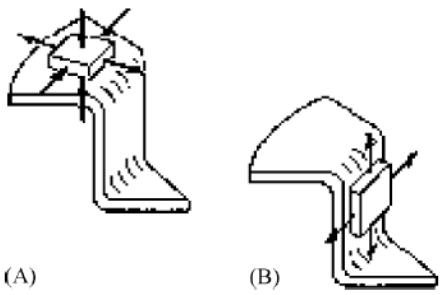

Figure 2.1: Workpiece stresses during deep drawing (Colgan & Monaghan, 2003)

In the deep drawing process, the drawing ratio, $\frac{D}{d}$ is dependent on the thickness ratio, $\frac{t}{D}$. This drawing ratio is related to the maximum thickness that can be achieved before tearing. There is also an approximate straight-line relationship between changes to the punch force concerning the drawing ratio. The punch force (F_p) can be represented in empirical form as shown below (Colgan & Monaghan, 2003):

$$F_p = \frac{\pi \sigma_Y}{\eta} \frac{d}{2} ln \frac{D}{d} \tag{2.1}$$

Figure 2.2 shows a partially drawn blank with typical shape characteristics and thickness variations. In the flange area, thickening and stretching will occur, while necking happens in the sidewall and just above the punch nose radius. Figure 2.2 also shows a possible area for necking formation. The drawn cup must be defect-free to demonstrate that this method has several advantages for commercial-scale manufacturing.

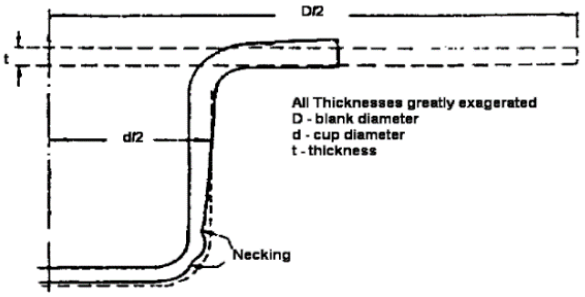

Figure 2.2: Deformation and necking of workpiece (Colgan & Monaghan, 2003)

Deep drawing operations can make products with good characteristics such as lightweight, thin, and higher strength products. But, meeting such demands will increase the chances of wrinkling and other defects (Singh & Agnihotri, 2015), even though the deep drawing process works better at higher temperatures.

2.3 Warm deep drawing

Warm deep drawing is a deep drawing process conducted within the warm thermal gradient to overcome the sheet metal material's low formability (Manabe et al., 2021). However, the warm thermal gradient introduced should be below the level of recrystallisation of the blank material.

From Bong et al. (2013), warm deep drawing is a conventional technique for enhancing the drawability of sheet metals. Based on trends, warm deep drawing offers several advantages over regular deep drawing. For example, better material flow and accomplished ideal parameters for a quality item include higher drawability, lower punch force, reduced fracture, and increased limiting drawing ratio (LDR) (Ethiraj & Kumar, 2012). In warm deep drawing, two strategies can be applied: ductility enhancement for warm materials and the effect of temperature gradients on material strength.

The material's drawability was increased during the warm deep drawing process because tool friction was controlled, where a deeper cup was formed (Desu et al., 2015). According to Zhang et al. (2006), the LDR increased significantly at warm than room temperature. On top of that, Kotkunde et al. (2020) also indicate LDR improvement from 1.8 to 2.13 at the forming temperature of 400°C . Previous studies used thermocouple or heating components to apply varied thermal gradients in constant temperature or heat transfer situations. For example, Manna and Mirzai (2019) used 5083 aluminium alloy in warm deep drawing experiment by heating the matrix and cooled the sheet's center.

Warm deep drawing uses various heating methods to warm the blank. From Martins et al. (2016), the blanks can be heated inside and outside the forming tools. Kou et al. (2021) used an assembled vacuum warm deep drawing apparatus to vacuum hot pressed the Ti/Al blank. Contrastly, Palumbo et al. (2007) used AZ31 magnesium alloy sheet in warm deep drawing by superimposing a heat gradient between the blank centre in contact with the punch and the blank flange.

2.4 The shape of the sheet metal drawn cup

Sheet metal drawing is a sheet metal forming method that uses punch force to distort the blank into the required shape, such as cylindrical, conical, rectangular, or square (Krupal et al., 2014). Shapes variety will have different characteristics and process parameter controls.

Hassan et al. (2014) investigate the square cups elongation by comparing experiment and FEA data. The effects of process factors such as die and punch corner radius, die throat length, shape factor, die clearance, and blank thickness on square cup drawability were investigated. The optimum parameters derived from the experiments were used in the FEA simulation, which showed that brass's LDR could be improved up to 3.1 and 3.15 for aluminium.

Moreover, Chen et al. (2003) also investigated square warm deep drawing's drawability. FEA was utilized to study the effect of punch and die corner radius and the forming temperature towards the drawability. A smaller punch radius reduces the drawability of square cup drawing, which is proven by relations between punch radius and drawn depth.

On the other hand, Ethiraj and Kumar (2012) studied the drawability of circular cups of austenitic stainless steel in the room and elevated temperature. The cup wall region is

examined to find fracture locations and compare the maximum drawing load. It concentrates on the effect of mechanical behaviour parameters towards the process.

Next, Manabe et al. (2021) investigate the drawability of the Zn-22Al-0.5Cu-0.01Mg alloy using experimental tests. The die flange area was heated and a set of variable punch speed and blank holding force was implemented. The effect of these variable parameters towards the flange wrinkle behavior were analysed.

2.5 Limiting drawing ratio (LDR)

Sheet metal drawing cylinder cups with high LDR are preferred to increase sheet metal drawing process capabilities and product quality. According to Banabic (2010), LDR is defined as the proportion between the greatest diameter of the workpiece that is deformed without tearing and the punch's diameter, given by:

$$LDR = \frac{D}{d} \tag{2.2}$$

Hassan et al. (2014) identify the effect of die corner radius, initial blank thickness, and die clearance will increase the LDR. On top of that, Moon et al. (2001) investigated the effect of tool temperature on the LDR of AL-1050 sheets and found the highest LDR by combining hot die at 200°C with a cold punch at -10°C. However, several temperature combinations can yield better results, and it concludes that tool temperature control is an effective way to increase LDR.

According to Naka and Yoshida (1999), the forming speed and temperature will incur positive results towards the LDR of the drawn cup. The LDR generally increases with temperature because the deformation resistance in flange shrinkage diminishes at rising temperatures. The flow stress of the heated blank increases with increasing strain rate, and the cooled blank at the punch corner becomes less ductile. As a result, at all temperatures, the LDR decrease as forming speed increase.

2.6 Drawability

The drawability of sheet metal is constantly related to material properties and can be determined through a tensile test. The drawability of a material is the measure of strain to which that material can be deformed before a fracture happens (Emmens, 2011). The tensile test is a fundamental material science test in which a specimen is subjected to a controlled tension until failure (Davis, 2004). The load-extension diagram and true engineering stress-strain diagram were products of the tensile test. The sheet metal's plastic and elastic deformation may be examined, and its drawability is calculated from this information.

The vital aspect of the load-extension diagram is the strain hardening. The sheet will have better performance with significant stretching if the straining is evenly distributed, as the sheet will resist tearing when the strain hardening is high. On the other hand, the initial yield strength is related to the strength of the formed part, especially where lightweight features are required. The higher the yield strength, the more efficient the material. The elastic modulus likewise influences the performance of the formed part, and a higher modulus will give a stiffer segment as an advantage. In terms of form, the modulus will affect the spring-back effect. A lower modulus gives a more significant spring-back effect and is typically more intricate in controlling the final dimensions (Marciniak et al., 2002).

The material with the same properties is measured in any direction is termed isotropic. However, most industrial sheets will distinguish in properties measured in test pieces aligned, for instance, with the coil's rolling, transverse, and 45° bearings. This variation is known as planar anisotropy. Moreover, there were differences in average properties in the sheet plane and through-thickness direction. In tensile tests of material that the features are the same in all directions, the width and thickness strains would be equivalent.

If they are distinctive, some anisotropy exists (Marciniak et al., 2002). A high value of normal anisotropy in deep drawing parts permits additional elements to be drawn. Increased normal anisotropy will reduce wrinkling or swells in shallow and easily moulded parts, such as automobile exterior boards.

Another significant consideration in drawability was the thickness distribution of the drawn cup and the punching force exerted. According to Colgan and Monaghan (2003), constant wall thickness is coveted. Subsequently, the smallest deviation from the average is required. The most minimal punch force was desirable as the higher is the punch force, the greater is the measures of wear on the tooling. Tool wear is a significant concern in industrial applications due to the expensive cost of replacing or repairing the tools. Laurent et al. (2015) found that the drawability of warm deep-drawn cup of Al-Mg alloy was affected by the anisotropy of the material, process temperature, and strain rate. A tensile test was used to identify these factors that affect drawability.

Other than that, Goud et al. (2014) utilize a load-displacement diagram to identify factors affecting the drawability of extra deep drawing steel at elevated temperatures. The diagram observed the relationship between the strain data points in the neck and fracture region with data points towards the biaxial stress line. In this study, the work hardening regime starts appearing between 350°C to 400°C, according to this diagram. There was also a slight increase in the work hardening coefficient and strength of the material in this temperature range.

Chen and Sowerby (1996) explained the earing behaviour in the circular deep drawing using the anisotropy concept. The study has shown that ideal blanks can be created for the deep drawing of circular cups, utilizing the strategy for plane strain characteristics without violating the Hencky conditions. The approach for plane strain characteristics can be used to predict four-fold symmetrical earing.

On the other hand, Colgan and Monaghan (2003) measure the drawability of deep-drawn cups using the thickness distribution and punch force. This study aimed to improve the deep drawing process by identifying the optimum value for the punch and die radii, punch velocity, clamping force, friction, and draw depth. Findings show that die corner radius affects the thickness distribution and punching force. The smaller the die corner radius, the greater punching forces exerted, causing severe thinning along the cup's wall.

2.6.1 Tools of the sheet metal drawing process

The sheet metal drawing process consists of several tool shapes, including circular, square, rectangular, and conical. For example, Pandre et al. (2021) analyse deep drawing of DP590 circular steel blanks into axisymmetric cylindrical cups using numerical modelling at different draw conditions. Besides that, Ogawa et al. (2016) described the drawability prediction by the computer simulation of the square cup deep drawing of pure titanium.

According to Dwivedi and Agnihotri (2015), the punch and die angle can affect the flow stress distribution, thus affecting the drawability of the drawn cup. For instance, Reddy et al. (2012) stated that the increment of the wrinkle height could be noticed when the small die radius is applied, while for the shorter drawn cup, the wrinkles have a greater amplitude as the die radius increases. Furthermore, according to Behrens et al. (2015), an increment in the die radius size cause a decrement in punch force when compared experimentally and numerically. From Tschaetsch (2004), the formula for calculating the die radius is:

$$r_M = \frac{0.035}{\sqrt{mm}}[50\ \text{mm} + (\text{D} - \text{d})]\,.\sqrt{s} \tag{2.3}$$

where r_M for die edge curvature, D for diameter of the blank, d for punch diameter, and s for sheet thickness.

The blank holder is associated with blank holding forces. For example, Marumo et al. (2007) stated the blank-holding force is affected by sheet thickness and the coefficient of friction. As the blank-holding force is varied during the process, there was no dramatic decline in LDR. Thus, LDR can be improved by manipulating the blank holding forces during deep drawing.

2.6.2 Punching speed

Punching speed was essential in the sheet metal drawing process, as sufficient punching speed allows the materials to flow through the tool within a certain period. Corner cracking will always occur in the sheet metal drawing process if the punch speed is too fast. Referring to Manabe et al. (2021), a maximum allowable punch speed produces a good cup in a shorter period. The study also suggests that increasing variable blank holding force along with the punch speed cause the wrinkling effect formed at the early stage of deep drawing process.

Optimal punching speed is desired as it affects deformation time, especially in industrial settings. The higher the punch speed, the faster the sheet metal deformation period. However, to achieve a short period of deformation, the capability of materials to flow, particularly the plastic strain ratio, must be considered first.

2.6.3 Thickness distribution

A uniform thickness distribution along the formed cup's wall is desirable results from deep drawing process. Various process parameter can contribute to this factor. For example, Kardan et al. (2018) finds that blank thickness, lubrication and die radius affect the thickness distribution the most. Furthermore, Younis (2013) stated that variable non-uniform blank holding force can produce a cup with uniform thickness.

Other than that, mechanical properties of the material also plays an important role towards uniform thickness distribution. For instance, Gao et al. (2009) studied the effect of material characteristic such as elastic modulus, yield stress, and hardening exponent towards thickness distribution and forming load. Not only that, FEA also being utilised to investigate this matter. Venkateswarlu et al. (2011) implement the FEA technique to determine the most significant parameter on drawability of aluminium alloy 7075 which is blank temperature.

2.7 Materials

The drawability of sheet metal is essential in fabricating sheet metal products. However, different sheet metals such as aluminium, mild steel, and stainless steel exhibit different material compositions and mechanical behaviour that affect their drawability.

Generally, aluminium inhibits several advantages such as lightweight, excellent strength to weight ratio, corrosion resistance and heat treatable. Compared to mild steel, it has superior drawability, a higher strength-to-weight ratio, is less expensive, and has better structural qualities after forming. On the other hand, stainless steel has advantages in corrosion-resistant, high strength to weight ratio, heat treatable, good wear-resistant, hardening very quickly, and has spring back characteristics.

2.7.1 Aluminium

Aluminium is a ductile metal with excellent drawability manufactured from bauxite. Although pure aluminium has poor strength, it can be alloyed and heat-treated. However, according to Ambrogio et al. (2005), precise sheet metal compositions and mechanical characteristics are required for simulation studies. Gavas and Izciler (2007) agree with this statement and conduct uniaxial tension tests to measure the tensile strength and examine the anisotropic behaviour of aluminium before running the experimental works of the deep drawing process.

2.7.2 Mild steel (Low carbon steel)

Low carbon steel or MS were widely used in many metal products. MS stampings have unique characteristics, benefits, and challenges in sheet metal drawing. MS contained less than 0.20% carbon and was relatively easy to form. MS is the most common metal used for sheet metal drawing forming, primarily due to the tremendous cost to performance attributes.

MS provides excellent drawability, which is also dependent on the specific grade of MS, as indicated by Meric et al. (1997). MS has good drawability when the thickness and deformation ratio rise, R values fall while n values grow. In addition to that, it has an excellent strength-weight ratio and can provide an outstanding structural characteristic after forming. The MS material was known to have a melting point of 1430°C and exhibits an elastic modulus of 200 GPa (Groover, 2013).

2.7.3 Stainless steel

Stainless steels are known for their strength and ductility. However, dealing with these alloys is challenging. In addition, compared to carbon steel or low alloy steel, stainless steel is more costly. Stainless steels can be categorized into austenitic, ferritic, and martensitic stainless steels (Groover, 2013).

Apart from that, Takuda et al. (2003) claim that austenitic stainless steel 304 is unstable and converts to martensite during cold forming. Deformation-induced martensite accelerates work-hardening, which is advantageous since it delays necking. However, the deformation-induced martensitic transformation also has an unfavourable influence. It needs several redrawing processes to obtain a sound cup. Due to the accumulated strain in multistage operations, the increased martensite concentration causes a rise in the working force, a loss in corrosion resistance, magnetization, and delayed cracking. Therefore, the annealing processes are necessary during and after the multistage sheet

metal drawing processes. Warm forming is advantageous for avoiding martensitic transformation and annealing operations since the martensitic transformation decreases with increasing temperature.

The stainless steel deep-drawn cup portrays good dimensional stability, hardens very quickly, and has spring-back characteristics. However, the distribution of flow stress depending on the temperature in the sheet will influence the drawability. Furthermore, even in a low-temperature range under 150°C, the flow stress of stainless steel 304 sheets fluctuates substantially. On the other hand, stainless steel has a melting point of 1400°C-1450°C and an elastic modulus of 193 GPa.

2.8 Design of experiment and quality characteristic analysis

In experimental works or manufacturing processes, it is crucial to identify and explore the relationship between the critical input process variables (factors) and output performance characteristics (response) (Antony, 2014). This phase is useful for statistically analysing parameters and planning the decision-making process. The factorial, surface response, and Taguchi methods were famous examples for the design of experiment approaches.

Each element's influence on the response variable is investigated in a full factorial experiment. Goud et al. (2014) applied the full factorial design to study the work forming limit diagram for extra deep drawing steel at room and elevated temperature. All possible combinations of a set of factors are carried out. However, if there are too many options, a complete factorial design is not viable due to the high cost and time factor.

As a result, the fractional factorial design was created to enhance experiment design by reducing the number of experiments by excluding some of the possible combinations.

A set of orthogonal arrays was proposed by Dr Genichi Taguchi, where fractional factorial designs were standardized (Roy, 2001).

2.8.1 Taguchi method

The Taguchi method is an orthogonal array approach to improve the quality of manufacturing processes. It is an optimal design approach for single quality characteristic projects that enables a fair comparison of process parameter levels and a significant reduction in the overall number of required runs (Kuo et al., 2019).

For example, Reddy et al. (2016) applied the Taguchi method and analysis of variance (ANOVA) to establish the best process parameters for AA6111 aluminium alloy based on their effect on thickness variation at various locations. Moreover, Kardan et al. (2018) utilize L27 orthogonal array to design the experiment and proceed with ANOVA to determine which parameter enable to reduce punch force and maximize uniform thickness distribution.

2.8.2 Signal-to-noise ratio analysis

Signal-to-noise ratio (S/N ratio) is the performance of uncontrolled parameters and process variables. It is used to determine the quality characteristic from the target, which involves using mean-square deviation (MSD). The S/N ratio has three instance applications, namely “Larger-is-the-best”, “Nominal-the-best”, “Smaller-is-better”. In deep drawing, examples of quality characteristics or response factors are punch microridge dimensions (Kuo et al., 2019), the maximum and minimum height of deep-drawn cup (Venkateswarlu et al., 2011), and thickness distribution (Reddy et al., 2016),

For the larger-is-the-best instance application, the related response factors were LDR, maximum and minimum height of the deep-drawn cup. For this response factor, a higher value is desired. Furthermore, the following response factor, thickness distribution, was

associated with nominal-the-best, aiming to have a uniform thickness along the deep-drawn cup profile. Smaller-is-better is suitable for the response factor of punching force as it desired to have the smallest punching force to deform the sheet metal. Consequently, the expression for evaluating these situations was defined by Taguchi is presented as follows:

$$\text{Larger-is-the-best: } S/N\ ratio = -10log\left(\frac{1}{n\left(\sum\frac{1}{y_i{}^2}\right)}\right) \tag{2.4}$$

$$\text{Nominal-the-best: } S/N\ ratio = 10log\left(\frac{\overline{y}^2}{s_y{}^2}\right) \tag{2.5}$$

$$\text{Smaller-is-better: } S/N\ ratio = -10log\left(\frac{1}{n(\sum y_i{}^2)}\right) \tag{2.6}$$

where y_i represents the measured response factor corresponding to the "*i* th" test, *n* is the number of samples in each test trial. S/N ratio is predicted at an optimum level using:

$$S/N_{predict} = T + \sum_{i=1}^{n}(F_i - T) \tag{2.7}$$

where *T* is the mean of total S/N ratio for optimum factor, *i* is the counter, and *n* represents the total number of experimental trials. A comparison of the predicted and experimental observed S/N is used to validate the method output. In addition to that, ANOVA is incorporated into the Taguchi Method to explicitly determine the effect and contributions of input factors considered on the response factor.

2.8.3 Analysis of Variance (ANOVA)

An ANOVA test is used to determine whether the findings of a survey or experiment are significant. In other words, the ANOVA test will decide if the null hypothesis should be rejected or the alternative hypothesis should be accepted. ANOVA divides an observed variable into two categories: random and systematic variables. The statistical method for ANOVA is described as follows.

Overall mean S/N ratio for *n* number of experiments is defined as:

$$\frac{\bar{S}}{N} = \frac{1}{n}\sum_{i=1}^{n}\left(\frac{S}{N}\right)_i \tag{2.8}$$

The total sum of square deviation, SS_T is expressed as:

$$SS_T = \sum_{i=1}^{n}\left(\left(\frac{S}{N}\right)_i - \frac{\bar{S}}{N}\right)^2 \tag{2.9}$$

For *yth* process parameter, the sum of square deviation is given by:

$$SS_y = \sum_{i=1}^{n}\left(\left(\frac{S}{N}\right)_{yz} - \frac{\bar{S}}{N}\right)^2 \tag{2.10}$$

where *z* is the number of levels of *y* factor.

The percentage distributions (ρ) of each variable is evaluated using:

$$\rho = \frac{SS_y}{SS_T} \times 100\% \tag{2.11}$$

The design and analysis of ANOVA can be implemented by using Minitab 17 statistical software.

2.9 Defects in the sheet metal drawing process

A defect is defined as a flaw or imperfection in the manufacturing components and can be classified based on physical characteristics. According to Banabic (2010), defects can be caused by forming tools, friction, geometrical factors, material mechanical and metallurgical qualities. The sheet metal drawing defects cannot be prevented, but reducing the probability is a priority. Common defects in sheet metal drawing were tearing, wrinkling, and earing.

Moreover, Ghafar et al. (2021) studied the thinning and tearing defect that was caused by the punch-die misalignment. Severe punch-die misalignment leads to increment of punch force. Eventually, it will produce cup with non-uniform wall thickness and increase the thinning pattern. In this study, single and multi-axis misalignment were considered.

On the other hand, Reddy et al. (2012) study the effect of blank holding force (BHF), punch radius, die edge radius, and coefficient of friction on the wrinkling of deep-drawn cylindrical parts. Findings show that increasing the BHF, lowering friction, increasing the tool's edge radius, and decreasing sheet metal drawing depth will minimise the wrinkles' height.

2.10 Finite element analysis (FEA)

FEA is a computer-aided technique for simulating how a product will react to forces, vibration, heat, fluid flow, and other physical influences in the actual world. FEA can predict whether a product will fail or perform as planned.

For example, Ambrogio et al. (2005) applied FEA to investigate the possibility of enhanced deep drawing formability after thermal gradient application. Besides that, Zhang et al. (2007) implemented FEA to study the effects of blank holding forces towards magnesium alloy blank's quality that undergo warm deep drawing. FEA commercial software such as ABAQUS/CAE, ANSYS, and PAM-STAMP was widely used in the sheet metal forming industry. It can analyse sheet metal drawability like thickness variation, height, and LDR.

Moreover, Saxena and Dixit (2009) utilise FEA to investigate the impact of tooling geometry and process parameters on earing formation in square and circular cup deep drawing. For circular cups, the material anisotropy affects the maximum ear height. In contrast, the metal flow rate at the square cup's vertical wall region is higher than the corner region. In this study, FEA predicts the drawability of sheet metal based on specific parameters to save time and money at the industrial tool design stage.

Additionally, the FEA simulation has 3D and two-dimensional (2D) visuals that aid audience comprehension. Sherbiny et al. (2014) use ABAQUS/EXPLICIT to simulate the

deep drawing process. It was defined with anisotropic material properties and simplified boundary conditions to forecast the blank's thickness distribution and maximum residual stresses at various die design parameters. Similarly, Singh et al. (2010) applied FEA visual tools advantage to investigate the LDR and the coefficient of friction of extra-deep drawing (EDD) steels at room temperature and 200°C.

FEA is also able to determine the best blank design to eliminate wrinkles. (Lee & Chun, 2005) use PAM-STAMP software to study the drawability of deep-drawn square SS304 cups at various temperatures. The outcome shows that uneven inflow of the blank between step edges caused the formation of wrinkles. This study compares the drawn cups from experiments and simulation to verify the FEA predictions.

2.11 Summary of literatures

Several research gaps have been discovered based on the literature studies on sheet metal drawing. Firstly, there were limited recent research references on a warm sheet metal drawing of square cups. Next, under the non-isothermal condition, heating techniques discussed in warm sheet metal drawing operation are restricted to certain boundaries. Most studies implement a more complex warm sheet metal drawing apparatus set up than a simple one.

This study intends to suggest a process improvement with minimal setup costs in existing manufacturing practices. The drawability improvement for the common steel will be observed by applying minimal thermal application to the process. Besides that, most of the existing sheet metal drawing process improvement approach is only suitable for specific alloy or niche products. Additionally, for circular and square sheet metal drawn cup, the comparison of thickness variation between FEA and experimental data were rarely discussed.

CHAPTER 3: RESEARCH METHODOLOGY

3.1 Research Methodology

The study aims to investigate the influence of die temperature on circular and square sheet metal drawing, evaluate the effect of process parameters on warm sheet metal drawing, and compare the drawability of sheet metal drawn circular and square cups using experiment and FEA data. Thus, the research design will include the details of the experimental setup apparatus, such as the tooling dimension, mechanical properties of the material, and process parameters. In addition, the role of ABAQUS/CAE and Minitab 17 will also be discussed.

The research design for this study is shown in Figure 3.1. It starts with the problem statement and research scope, leading to literature reviews relevant to the research scope. Then, using the Taguchi method, the study's process parameters and experimental design were determined and designed. Following that, the experimental process was planned for circular and square cups. The experimental apparatus consists of die sets, heaters, thermocouples, hydraulic pump and cylinder. The setup and procedures must be tested to ensure the intended output can be recorded using the Taguchi method. After confirmation, actual experiment runs will be conducted, and FEA is performed using ABAQUS/CAE to predict the drawability of the drawn cup. The experimental runs and the FEA data will be tabulated and analysed. The output from FEA and experiment will be statistically analysed using ANOVA and the S/N ratio approach utilizing Minitab 17 software. However, if the results are not satisfying, the process will repeat, starting from the experimental and FEA stage.

Finally, the data that could satisfy the stated objectives will be discussed and documented. A complete report will be provided at the end of the study.

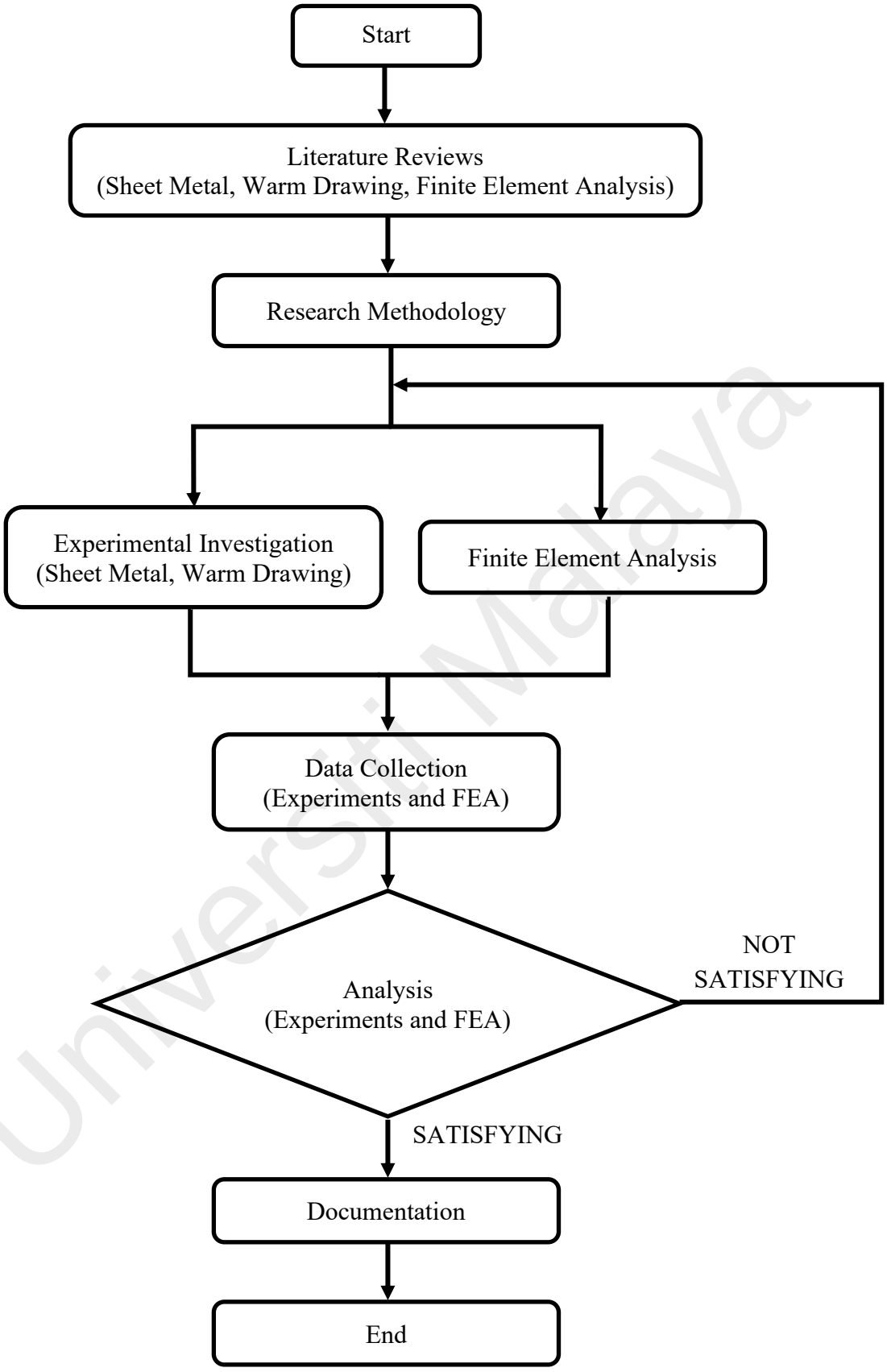

Figure 3.1: Research Design

3.1.1 Experimental setup

Figure 3.2 shows the experimental setup for the warm and room temperature sheet metal drawing process. The setup consists of a single-acting hydraulic cylinder, a hydraulic pump, a die set attached to the die shoe, a set of thermocouples and heater connected to the temperature controller, and finally, the insulated force sensor with a data acquisition system.

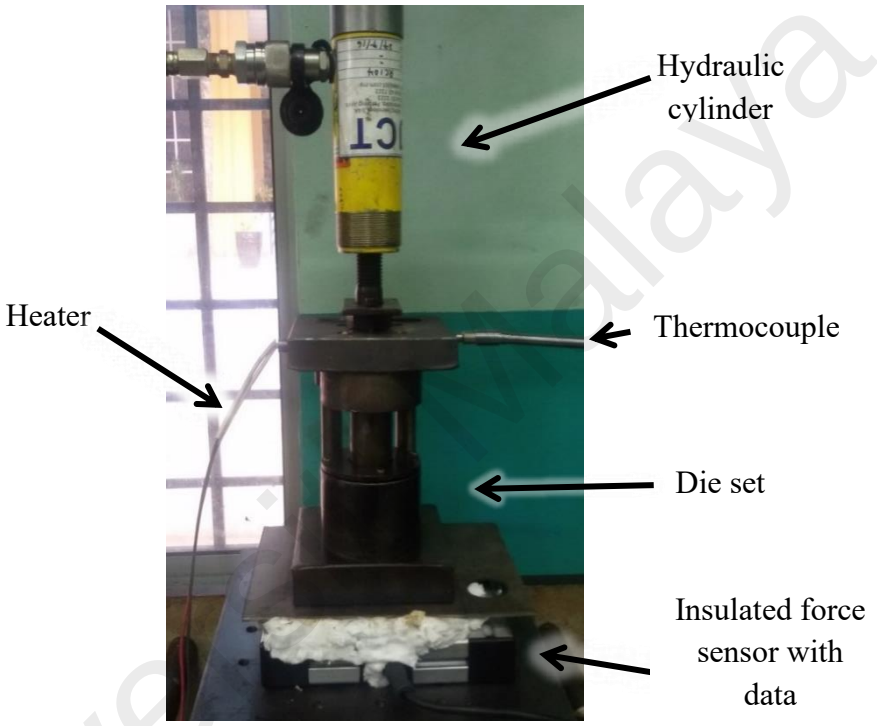

Figure 3.2: Experimental setup for warm and room temperature sheet metal drawing

The Enerpac RC-104 single-acting hydraulic cylinder uses pressurised fluid to generate the punching force. The specification of the RC-104 hydraulic cylinder is shown in Table 3.1.

Table 3.1: Specification of hydraulic cylinder *(source: http://www.enerpac.com)*

Model No.	RC-104
Cylinder capacity (kN)	101
Stroke length (mm)	105
Cylinder effective area (cm^2)	14.5
Oil capacity (cm^3)	152
Collapsed height (mm)	171
Weight (kg)	3.3

A Royal Master hydraulic pump unit operated using reliable remote control equipped with a solenoid valve. It uses pressurized fluid to move the hydraulic cylinder and overcome the load resistance.

A heating instrument set consists of a temperature controller, heater, and thermocouple. The temperature controller regulates the heat for the die set at a specified temperature. The thermocouple detects temperature changes in the medium and delivers the signal to the temperature controller. Once the specified temperature is achieved, the temperature level will be maintained.

From Figure 3.2, the force sensor with the data acquisition system consists of a force sensor, data logger, and digital indicator. First, the force sensor detects the punching force from the sheet metal drawing process. Next, the force is converted into a micro voltage signal through the Wheatstone bridge principle contained in the force sensor. Then, the signal is amplified and transferred to the data logger and digital indicator situated in the main box. The data logger can record the current value until one reading per second and store it directly to the device memory. The data can be extracted using a USB and analysed using the software. The digital indicator contains calibration tools and shows a live display of the punching force reading. The system is equipped with insulation to work in a high-temperature environment. Table 3.2 shows the specification for the system and the force sensor.

Table 3.2: Specification for force sensor with the data acquisition system

Force sensor (Load cell)	Maximum capacity (ton)	20
	Operating temperature (°C)	-20 to 65
	Safe load limit (%)	200
	Ultimate load (%)	300
	Sensitivity (mV)	±0.05
	Rated Output (mV)	2 ± 0.1
	Dimension (D x H) (mm)	120 x 54
	Material	Stainless steel 17-4 PH
Data Logger	Power supply voltage (V)	16V AC
	Display	Graphic LCD
	Transmission speed (bit/sec)	1200 – 115200
	Memory capacity (MB)	2
	USB connection	Yes (IP 40)
	Working temperature (°C)	0 - 60
	Dimension (W x H x L) (mm)	96 x 96 x 100
Digital Indicator	Input range (mV)	0 ± 20
	Sensitivity (μV/digit)	0.5
	Display	LED

The Dino-Lite Premier AM7013MZT4 digital microscope measured the wall thickness distribution. It can zoom and digitally focus on the image of the dissected sheet metal drawn cup to ensure measurement precision.

In this study, the temperature difference was applied to enhance the drawability of the drawn cup. A FLIR i7 thermal imaging camera was utilised to show the blank's heat map. It is essential to ensure that the blank's temperature is met before starting the process.

3.1.2 Die set for circular cup

Figure 3.3 illustrates the circular cup's tools set consisting of upper and lower die shoe, punch, die and blank holder. The upper and lower die shoes ensure the blank is concentric with the die cavity while linearly guiding the punch and die. The heater and thermocouple are installed in the die shoe to heat the punch and die. A full blank holder with fasteners was used to compensate for residual tensions that may cause wrinkling.

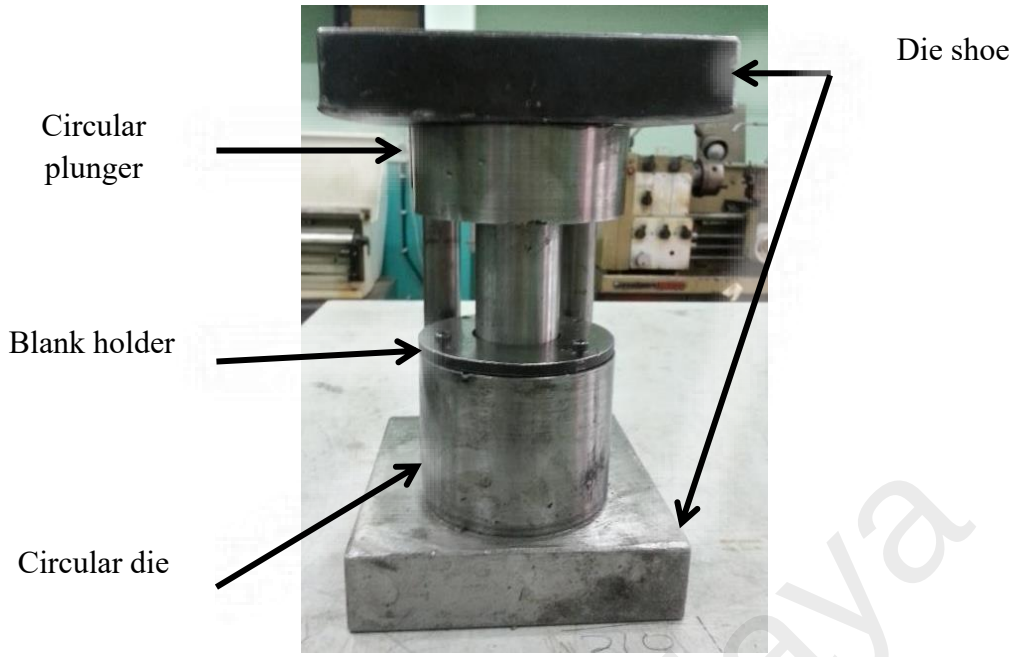

Figure 3.3: Circular die set

In this study, due to the differences in die throat tolerance for various blank materials, two sets of tools comprising a plunger and a die were employed. There are two sets of tools: one for AL6065 and MS blanks and another for SS304 blanks exclusively. The tooling dimensions for sheet metal drawing processes employing various materials are shown in Table 3.3.

Table 3.3: Tooling dimension for circular blank

Die (Circular AL6065 and MS blank)	Height (mm)	70.00
	Inner diameter (mm)	40.40
	Per side clearance (mm)	1.07
	Outer diameter (mm)	90.00
	Die throat corner radius (mm)	5.00
Die (Circular SS304 blank)	Height (mm)	70.00
	Inner diameter (mm)	41.06
	Per side clearance (mm)	1.40
	Outer diameter (mm)	90.00
	Die throat corner radius (mm)	5.00
Punch	Height (mm)	60.00
	Diameter (mm)	38.30
	Punch corner radius (mm)	5.00
Blank Holder	Thickness (mm)	5.00

3.1.3 Die set for square cup

Figure 3.4 shows the square cup's tools set consisting of upper and lower die shoe, blank holder, square punch, and die. The tooling dimensions for the square cup are described in Table 3.4.

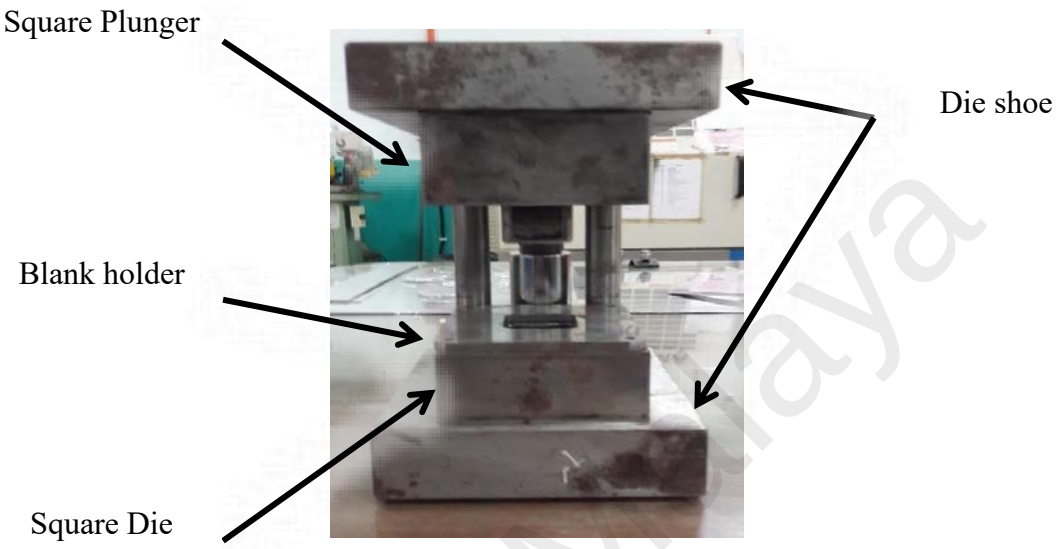

Figure 3.4: Square die set

Table 3.4: Tooling dimension for square blank

Die	External Length (mm)	90.00
	External Width (mm)	90.00
	Length (mm)	34.50
	Width (mm)	34.50
	Height (mm)	35.00
	Corner radius (mm)	2.00
Punch	Length (mm)	32.50
	Width (mm)	32.50
	Height (mm)	20.00
	Corner radius (mm)	2.00
Holder	Length (mm)	34.50
	Width (mm)	34.50
	Height (mm)	5.00

3.1.4 Material selection

This study used AL6065, MS, and SS304 as the blank materials because of their low cost, mechanical, and thermal qualities. The details of the material properties specifications are tabulated in Table 3.5.

Table 3.5: Mechanical and thermal properties of aluminium 6065, MS, and SS304 (Groover, 2013)

		AL6065	MS	SS304
Mechanical properties	Modulus of elasticity (GPa)	69	200	200
	Yield strength (MPa)	105	250	215
	Ultimate tensile strength (MPa)	110	400-550	505
	Hardness, Brinell (HB)	30	120	123
Thermal properties	Specific heat capacity (J/g °C)	0.9	0.51	0.5
	Thermal conductivity (W/mK)	227	50	16.2
	Melting point (°C)	646-657	1450	1400-1455

3.1.5 Design of experiment using Taguchi approach

Design of experiments (DOE) is a quantitative and efficient way to determine the effects of several variables simultaneously. It is used to investigate the relationships between conditions and logical outcomes in a situation.

The Taguchi method is commonly used to investigate the effect of parameters on sheet metal drawing performance. It is a standardised and straightforward strategy for reducing experimental costs and time by eliminating numerous possible parameter combinations from a full factorial approach. As a result, the output quality can be improved and optimized by deciding the best combination of the variables. The flow of the process for the Taguchi approach was as follows:

1. Phase I: Plan of Experiment
    - The objectives of the study have been clarified.
    - Quality characteristics and measurement methods have been decided.
    - Identify and choose process parameters that will impact the output outcome.
    - Select the levels for each factor involved.
2. Phase II: Designing the experiments
    - The orthogonal array is selected based on the number of factors and levels.
    - Factors and levels are assigned to the orthogonal array.
3. Phase III: Conducting the experiments
    - Several samples must be obtained for each condition is conducted for the experimental runs.
    - Data collection.
4. Phase IV: Analysing the results
    - Identify the significant factors.
    - Determine the optimal conditions.
5. Phase V: Designing the experiments
    - A confirmation test is carried out to verify the performance at optimum conditions.

3.1.6 Experiment's parameters

The material, shape of the drawn cup, temperature, blank size, and heating processes are control elements in this study. Therefore, the study will emphasise how these control elements affect material drawability in the warm sheet metal drawing process. Table 3.6 and Table 3.7 indicate the levels of each component for circular and square warm sheet metal drawing, respectively.

Table 3.6: Selected factors and levels for circular sheet metal drawing

Factors	Level		
	1	**2**	**3**
Material	AL6065	MS	SS304
Blank size (mm)	60	65	70
Temperature (°C)	100	150	200
Heating techniques	Die	Punch	Die and punch

Table 3.7: Selected factors and levels for square sheet metal drawing

Factors	Level		
	1	**2**	**3**
Material	AL6065	MS	SS304
Blank size (mm)	45	50	55
Temperature (°C)	100	150	200
Heating techniques	Die	Punch	Die and punch

3.1.7 Orthogonal array

There were four control variables in this study, each with three levels. As a result, the L9 orthogonal array was selected as the design of experiments. Table 3.8 shows the L9 orthogonal array built using the Taguchi method. Consequently, Table 3.9 tabulated all control parameters for circular and square warm sheet metal drawing into the L9 orthogonal array.

Table 3.8: L9 Orthogonal array

Experiment No.	Factor 1	Factor 2	Factor 3	Factor 4
1	1	1	1	1
2	1	2	2	2
3	1	3	3	3
4	2	1	2	3
5	2	2	3	1
6	2	3	1	2
7	3	1	3	2
8	3	2	1	3
9	3	3	2	1

Table 3.9: L9 Orthogonal array for circular and square sheet metal drawing in warm condition

Experiment No.	Material	Blank size for circular sheet metal drawing (mm)	Blank size for square sheet metal drawing (mm)	Temperature (°C)	Heating Technique
1	AL6065	60	45	100	Die
2	AL6065	65	50	150	Punch
3	AL6065	70	55	200	Die and Punch
4	MS	60	45	150	Die and Punch
5	MS	65	50	200	Die
6	MS	70	55	100	Punch
7	SS304	60	45	200	Punch
8	SS304	65	50	100	Die and Punch
9	SS304	70	55	150	Die

All three circular and square cup materials will be drawn for the experimental controls at room temperature. Therefore, it is essential to compare room and warm sheet metal drawing output. The experimental conditions for circular and square cup sheet metal drawing at room temperature are described in Table 3.10. Each drawn cup shape will be repeated three times based on these tables to acquire the average results.

Table 3.10: Experiments for circular and square sheet metal drawing at room temperature

Experiment No.	Material	Blank size for circular sheet metal drawing (mm)	Blank size for square sheet metal drawing (mm)
1	AL6065	60	45
2	AL6065	65	50
3	AL6065	70	55
4	MS	60	45
5	MS	65	50
6	MS	70	55
7	SS304	60	45
8	SS304	65	50
9	SS304	70	55

3.1.8 Procedures

In this study, the experimental procedures are as follows:

1. For the blank samples, 1.0 mm thick AL6065, MS, and SS304 sheets were cut into circular and square shapes. Circular blanks have 60 mm, 65 mm, and 70 mm diameters, whereas square blanks have dimensions of 45 mm, 50 mm, and 55 mm. Figure 3.5 shows examples of circular and square blanks of various sizes.

Figure 3.5: Blank samples with different sizes for circular and square sheet metal drawing

2. The sheet metal drawing processes are conducted based on the L9 orthogonal array. First, the blank is placed on the die and held by a blank holder and die punch. Then, the blank temperature is verified using a FLIR i7 thermal imaging camera during the heating process. After the desired temperature is reached, the warm sheet metal drawing process is conducted.
3. The hydraulic pump and cylinder are activated using the controller, moving the punch downwards and pushing the blank into the die cavity.
4. The deformed cup is collected, and the average cup height is measured. Then, the defects such as tearing, earing, and wrinkling were observed and recorded.
5. Next, the LDR is calculated after recording the largest drawn blank size.
6. Lastly, the drawn cups were dissected, and the burr was cleaned. Then, the

Dino-Lite Premier AM7013MZT4 digital microscope evaluated the thickness variation along the cup's wall. Finally, the reading is recorded and tabulated.

3.2 Data collection and analysis

In this study, the quality measurement data has been collected and statistically analysed using analysis of variance methods. Lastly, the FEA simulation model is constructed to verify and compare the experiment's results.

3.2.1 Quality measurement methods

In this study, the quality characteristics measured are average cup height, LDR, thickness distribution, and the overall appearance of the drawn cup. These qualitative attributes were selected to evaluate the sheet metal drawn cup's drawability in a warm and room temperature sheet metal drawing. The maximum allowable error percentage were set at 25%. Table 3.11 illustrates the descriptions of quality measuring methodologies.

Table 3.11: Quality measurement methods

No.	Quality Characteristic	Description
1.	Average cup height	Height at different positions of the formed cup is measured, and the average value is calculated. A higher cup's height shows better drawability.
2.	Limiting drawing ratio (LDR)	The ratio of a cup's maximum blank diameter to its punch diameter can be drawn effectively. Therefore, higher LDR indicates higher drawability.
3.	Thickness distribution	Thickness at a different region along the sheet metal drawn cup's profile is measured. Thicker punch corner and uniform thickness distribution on the wall of sheet metal drawn cup show better drawability.
4.	Appearances of drawn cups	Justification of drawn cups quality. Defects such as wrinkling, tearing, earing and surface scratch on the sheet metal drawn cups were observed. Therefore, drawn cups with the least defects are desired.

3.2.2 Analysis of variance (ANOVA)

The ANOVA is used to determine which factors substantially influence the sheet metal drawing process's drawability and compute each parameter's contribution. ANOVA used mean squared deviation (MSD), which combines average and standard deviation effects. It is performed with an S/N ratio to compare the effect of parameters. S/N ratio is a logarithmic transformation of MSD. S/N for different quality characteristics are defined as smaller-the-better, bigger-the-better, and nominal is the best.

The ANOVA and S/N ratio will be analysed using Minitab 17 software in this study. Thickness distribution was selected as a quality characteristic with nominal-the-best S/N ratio. It suggests that the best output condition is the S/N ratio closest to the initial blank thickness of 1 mm. At first, the main effect plot for the S/N ratio will compare the factors that affect the response characteristic such as material, blank size, temperature, and heating technique. Consequently, Minitab 17 will yield the response table for the S/N ratio, and the factor with the highest delta value has the most impact on the drawn cup's thickness distribution. The optimal condition was determined by the peak point of the main effect plot and response table for each factor category. After that, the ANOVA analysis will calculate the sum of squares due to the variation from the average S/N ratio for the yth factor, SS_y. Finally, it is used to determine the contribution of each process parameter to yield the cup with optimal thickness distribution.

3.2.3 Finite element analysis (FEA)

ABAQUS/CAE simulation tool can simulate the sheet metal drawing process and change process parameters to forecast the ideal forming condition. It benefits from eliminating trial and error approaches to the manufacturing process, saving time and money. Furthermore, it can anticipate the influence of sheet metal drawing process factors on thickness distribution, stress-strain distribution, and defects in drawn cups. This tool can also exhibit cup formation animations in 2D and 3D.

Initially, an ABAQUS 3D model of the apparatus setup, which included a punch, blank holder, die, and blank sheet was created. The blank is placed between the blank holder and the die. Then, the material properties parameter such as density, Young's modulus, Poisson ratio, and strain hardening relation was defined. In addition, the friction coefficient (approximately 0.1) and punch speed were constantly defined in this study. Following that, two simulation stages were implemented. The first stage was the blank holding phase, in which the blank holder used a constant load to retain the blank while the punch became tangent to the blank. Next, the punch moves steadily toward the blank and deforms it until a depth of 25 mm, based on the average cup height discovered in the experiment. This step was considered to measure the thickness distribution from ABAQUS and will be compared to the experimental result.

For both circular and square sheet metal drawn cup, in general, the steps for the ABAQUS simulations are:

1. Define the sheet dimension and configuration. Makesure it is solid and deformable. The top and bottom surface were assigned.
2. Define the die dimension and configuration. Makesure it is discrete rigid and under shell criteria. The reference point and surfaces were defined.

3. Define the blank holder dimension and configuration. Makesure it is discrete rigid and under shell criteria.The reference point and surfaces were defined.
4. Define the punch dimension and configuration. Makesure it is discrete rigid and under shell criteria. The reference point and surfaces were assigned.
5. Under Assembly, an Instance were created for Die, Blank holder, Punch and Sheet. Dependent has been selected as the instance type.
6. Set the material properties for the blank and create the material profile. The parameters for density, Young modulus, Poisson ratio, yield strength, strain hardening exponential, hardening coefficient and hardening relation being defined.
7. Then, the mechanical properties of the material is added into the profile by defining the elasticity and plasticity criteria of the material.
8. The interaction profile then created by defining the friction coefficient of the lower die (0.05), blank holder (0.08), punch (0.1). Penalty contact method were assigned as the mechanical constraint formulation. The interaction between Holder-Sheet, Punch-Sheet, and Die-Sheet being defined and the mechanical properties of these interaction were assigned.
9. The step of the simulation consisting punch velocity movement inwards and outwards were input as 200 m/s.
10. The load were define for each of the interaction by defining under the Boundary condition (BC). BC were defined for the sheet side surface, punch velocity, die, holder, and punch displacement.
11. BC1 and BC2 were defined as symmetry and assigned to sheet side surfaces. Next, BC3 defined as displacement/rotation and assigned to die reference point. BC4 defined as displacement/rotation and assigned to blank holder reference point. BC5 defined as displacement/rotation and assigned to punch reference

point. Then, BC6 defined as velocity and assigned punch reference point.

12. Similar procedure were repeated for unloading mechanism of the sheet metal drawing process.
13. Next, the mesh of all parts were defined. The element type of 4 node 3D bilinear rigid quadrilateral were assigned to die, blank holder and punch with approximately global size of 1. The element type was explicit discrete rigid element.
14. For sheet, the element type of 8 node linear brick and 4 node linear tetrahedron were assigned. The approximate global size was 1 and explicit 3D stress element were assigned.
15. Finally, the meshing for all the parts were assigned and defined. The simulation were run and the thickness distribution along the cup wall were observed.

CHAPTER 4: RESULTS AND DISCUSSION

4.1 Introduction

This chapter presented the results obtained from circular and square cup sheet metal drawing experiments at warm and room temperatures. The results and discussions were based on the effect of temperature on the performances, such as LDR, average circular cup height, and thickness distribution. Then, the S/N ratio and ANOVA were applied to determine the effect of different process parameters. The drawability of the cup from the experiment and FEA will be compared.

4.2 Circular sheet metal drawn cup

4.2.1 Limiting drawing ratio (LDR) for the circular cup

The outcome of each experiment is observed and recorded. The circular cups formed in the room and warm sheet metal drawing are shown in Appendix A**.** Table 4.1 shows LDR for circular cups of AL6065, MS, and SS304 in the room and warm conditions.

The maximum LDR for MS and SS304 in the warm sheet metal drawing was 1.83, while AL6065 was 1.70. Meanwhile, the maximum LDR is 1.83 for all three materials in sheet metal drawing at room temperature. According to Table 4.1, for 70 mm blank diameter, only AL6065 blank fails to deform at warm sheet metal drawing due to tearing.

Table 4.1: LDR for circular cups of AL6065, MS and SS304 in the room and warm sheet metal drawing

Exp no.	Material	Blank size (mm)	Temperature (°C)	Heating technique	Results	LDR
1	AL6065	60	100	Die	Successful	1.57
			Room temp	N/A	Successful	1.57
2		65	150	Punch	Successful	1.70
			Room temp	N/A	Successful	1.70
3		70	200	Die & Punch	Failed	-
			Room temp	N/A	Successful	1.83
4	MS	60	150	Die & Punch	Successful	1.57
			Room temp	N/A	Successful	1.57
5		65	200	Die	Successful	1.70
			Room temp	N/A	Successful	1.70
6		70	100	Punch	Successful	1.83
			Room temp	N/A	Successful	1.83
7	SS304	60	200	Punch	Successful	1.57
			Room temp	N/A	Successful	1.57
8		65	100	Die & Punch	Successful	1.70
			Room temp	N/A	Successful	1.70
9		70	150	Die	Successful	1.83
			Room temp	N/A	Successful	1.83

Warm sheet metal drawing for 70 mm AL6065's blank was performed at 200°C by heating both die and punch. The AL6065 blank's yield and tensile strength decrease as the temperature rises, reducing drawability. Compared to MS and SS304, AL6065 has the weakest yield and tensile strength. Furthermore, since the heater was placed in die shoe, it took almost two hours for the blank temperature to reach 200°C. Even though the heat difference between the flange area and the blank centre during this heating process is relatively small, as hot punch forces blank into the die cavity, the strength of the blank at its centre is decreased. In addition, considering the high-stress concentration at the punch corner, this region loses a substantial amount of thickness and leads to thinning on the cup's wall. The thinning eventually develops, causing tearing defects as the punch travels further to push the blank into the die cavity.

4.2.2 Average circular sheet metal drawn cup height

The average sheet metal drawn circular cup's height according to the blank sizes for AL6065, MS, and SS304 in the room and warm sheet metal drawing is presented in Figure 4.1. The tabulated data of the average height of all drawn materials are recorded in Appendix A.

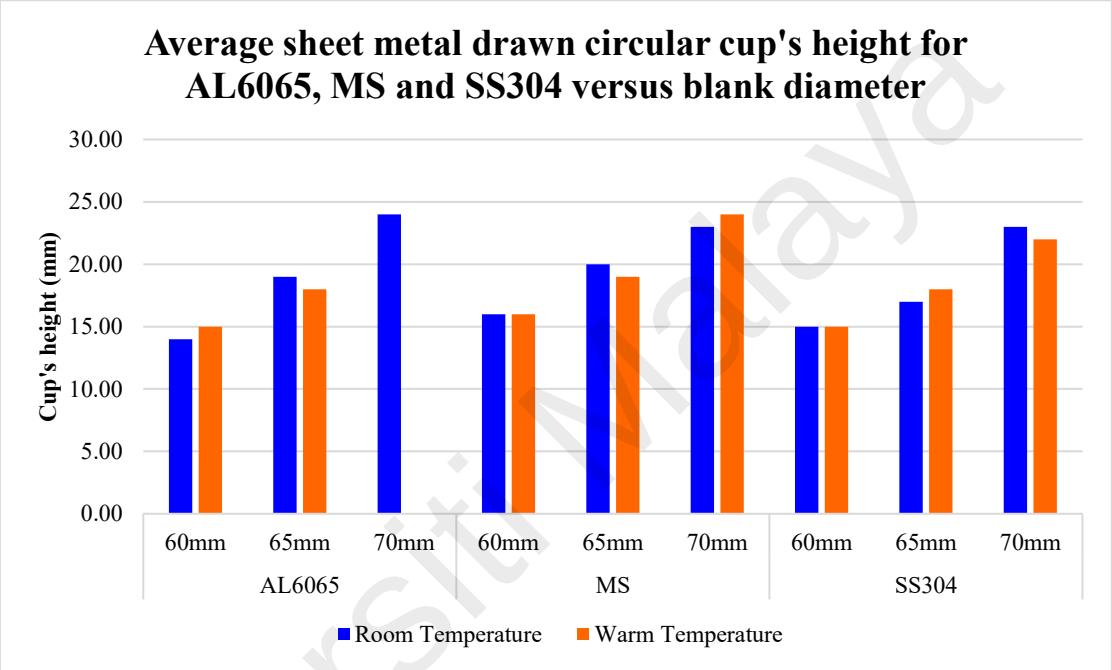

Figure 4.1: Average sheet metal drawn circular cup's height for AL6065, MS, and stainless versus blank diameter

The difference in cup height was referred to as earing, and the amplitude of the earing varies with the planar anisotropy coefficient. According to Vrh et al. (2013), an earing defect is the formation of waviness on the uppermost part of a sheet metal drawn cup. Therefore, the earing defect was usually trimmed after the sheet metal drawing process.

From Figure 4.1, the average cup height in warm sheet metal drawing was improved for 60 mm AL6065's blank, 70 mm MS's blank and 65 mm SS304's blank compared to room temperature sheet metal drawing. Contrastly, the average cup height of 70 mm SS304 blanks, 65 mm AL6065, and MS blanks decrease. However, the drawn cup's

height difference from the room and warm temperature is considered small, around 1.00 mm. Thus, the effect of temperature on the average height of a circular cup is negligible.

4.2.3 Thickness distribution of the circular cup

Thickness distribution is a vital drawability factor in sheet metal forming. The thickness is often homogeneous at the punch's bottom face, minimal at the punch nose radius and vertical surface, and thicker at the flange area. In this study, the thickness distributions were measured starting from the edge of the cup wall to the bottom centre, as shown in Figure 4.2. Before measuring the thickness distribution, the sheet metal drawn circular cup is dissected and the extra burr removed. It was measured using a Dino-Lite Premier AM7013MZT4 digital microscope, and twenty-five (25) points were recorded along the drawn cup's cross-sectional area. The thickness distribution of the drawn cup in the room and warm sheet metal drawing was presented in Figure 4.3. The tabulated data can be referred to Appendix B.

Figure 4.2: Illustration of measuring position along the circular cup's profile

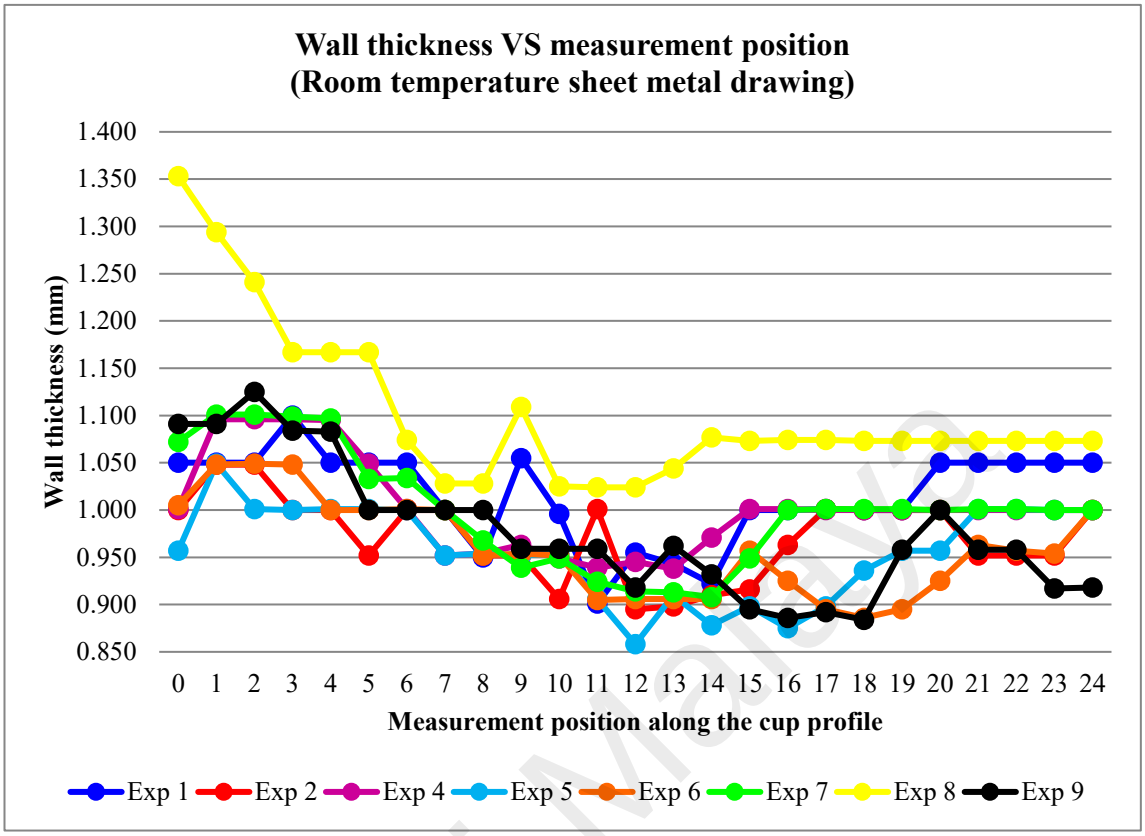

(a)

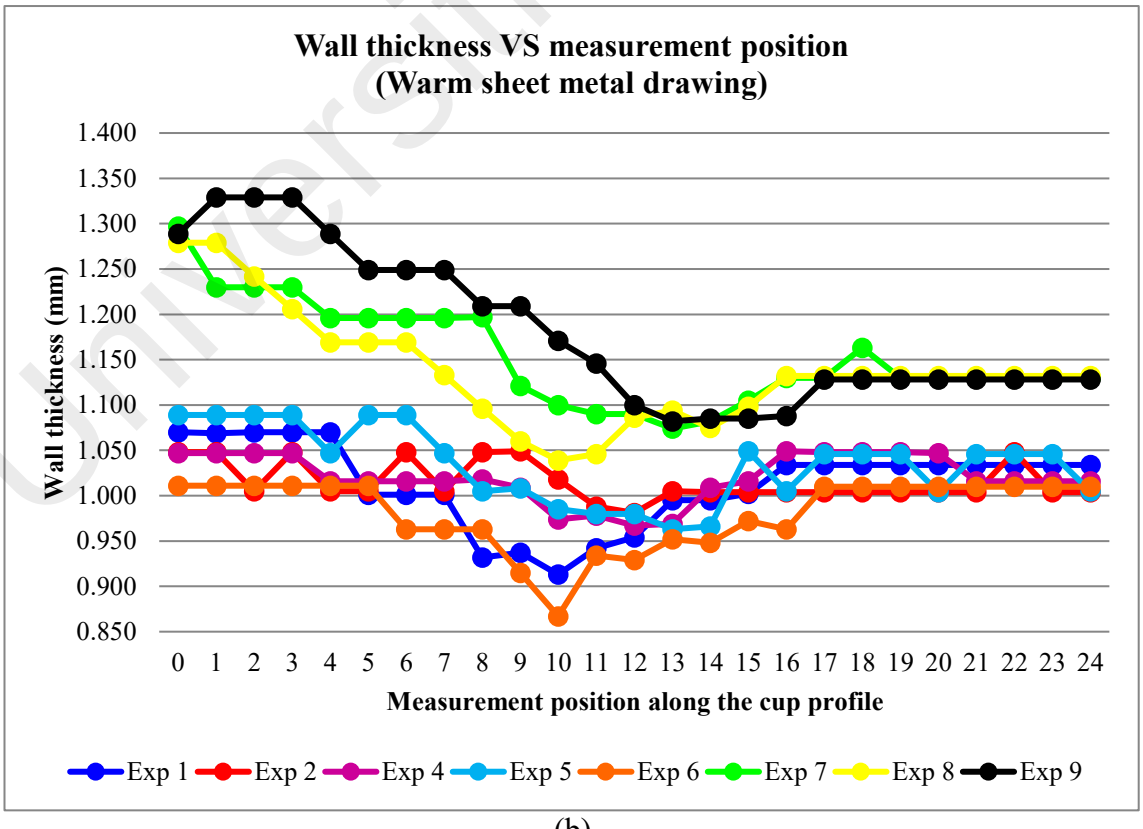

(b)

Figure 4.3: Thickness distribution along the circular cup profile in the sheet metal drawing process conducted at (a) room temperature and (b) warm temperature

In Figure 4.3 (a) and (b), Experiment 3 was not included as the cup failed to form in warm sheet metal drawing due to tearing. However, Figure 4.3(a) and Figure 4.3(b) showed thickening at the flange, thinning at the vertical surface and punch radius and consistent thickness at the punch's bottom face. There was insufficient stress for the circular cup's bottom face area to create a permanent deformation, making the thickness uniform and almost similar to the initial blank thickness. The warm sheet metal drawing yields more consistent bottom cup thickness in all experimental runs than the room temperature sheet metal drawing. In addition, in room temperature sheet metal drawing, the drawn cup suffers severe thinning at the punch corner than warm sheet metal drawing.

The cup’s punch corner experiences thinning due to the high-stress concentration in this area. Therefore, the material in this location will first bend around the die radius, then unbend when pulled against the die wall under tensile stress. After that, it continues to bend in the other direction around the punch corner. As a result, this region is prone to extreme thinning, leading to tearing defects, as seen in Experiment 3.

The thickness variation is caused by limited material flow into the die cavity, especially in room temperature sheet metal drawing. On the other hand, thickening happens at the flange area as the material experiences compressive stress and circumferential shrinkage. Therefore, minor wrinkling is unavoidable in this region, causing the thickening around the top edge of the cup’s wall. Further analysis will compare the standard deviation and minimum thickness for the cup drawn in the room and warm temperature, as shown in Table 4.2. The detailed graph and descriptive numerical table can be referred to Appendix B.

Table 4.2: Analysis of thickness distribution in circular sheet metal drawing experiment

Material	Exp	Temperature and heating technique	Standard deviation (mm)	Percentage difference for standard deviation (%)	Minimum thickness (mm)	Percentage difference for minimum thickness (%)
AL6065	1	RT	0.049	5.87	0.901	1.32
		100°C; Die	0.046		0.913	
	2	RT	0.043	63.93	0.895	9.17
		150°C; Punch	0.022		0.981	
	3	RT	N/A	N/A	N/A	N/A
		200°C; Die & Punch	N/A		N/A	
MS	4	RT	0.049	63.21	0.938	3.04
		150°C; Die & Punch	0.026		0.967	
	5	RT	0.050	19.29	0.858	11.53
		200°C; Die	0.041		0.963	
	6	RT	0.050	24.88	0.886	2.17
		100°C; Punch	0.039		0.867	
SS304	7	RT	0.059	4.95	0.908	16.75
		200°C; Punch	0.056		1.074	
	8	RT	0.084	30.39	1.024	1.45
		100°C; Die & Punch	0.062		1.039	
	9	RT	0.069	18.91	0.884	20.14
		150°C; Die	0.084		1.082	

Standard deviation is a metric for calculating the amount of variation or dispersion in a set of data values. A low standard deviation indicates that the data points are clustered around the set's mean. In contrast, a high standard deviation indicates that the data points are spread throughout a wider range of values. Consequently, when the circular cup's thickness distribution has a lower standard deviation, the thickness is typically near the mean and less dispersed. Hence, the thickness is distributed more uniformly.

From Table 4.2, most warm sheet metal drawing experiments provide a lower standard deviation for the cup's wall thickness than the room temperature sheet metal drawing. It demonstrates that the thickness variation in the warm sheet metal drawing is

typically nearer to the mean and less dispersed. All the drawn cups from warm sheet metal drawing have improved thickness distribution compared to room temperature sheet metal drawing, except Experiment 9. However, the standard deviation difference for Experiment 9 in the room and warm sheet metal drawing is only 18.91%. Even though the improvement was not fulfilled even after the thermal gradient was introduced, the thickness deviation was not severely scattered.

Both heating temperature and heating techniques improve the wall thickness distribution along the cup's profile. The most significant standard deviation improvement is found in Experiment 2 and 4, when a heating temperature of 150°C is applied to 65 mm AL6065 and 60 mm MS blanks. Moreover, the heating technique for Experiment 4 was at die and punch, while Experiment 2 was only at the punch. The heating temperature and technique manage to introduce the annealing effect, which causes decrement of the tensile strength and increment of the uniform elongation (Herrmann & Merklein, 2018). On the other hand, Experiment 7 has 4.95%, and Experiment 1 has a 5.87% standard deviation difference for room and warm sheet metal drawing. Both were deemed minor standard deviation improvements that can be further improved.

Meanwhile, the minimum thickness that frequently happens at the punch corner region has improved in all warm sheet metal drawings except Experiment 6. However, the percentage difference between room and warm sheet metal drawing was 2.17% and relatively small. As 70 mm was the largest blank size for the MS, the heating temperature and methods were insufficient to improve the minimum thickness.

Furthermore, in Experiments 1, 8, and 4, there is a minor improvement in the percentage difference for minimum thickness between the room and warm sheet metal drawing. It indicates

that even though the thickness distribution is improved by implementing heating conditions, it is relatively small and almost insignificant.

The best minimum thickness improvement happens at Experiment 9, as the percentage difference between room and warm sheet metal drawing increased by 20.14%. However, as mentioned earlier, the standard deviation for Experiment 9 has a significant percentage difference, which indicates the thickness distribution is dispersed widely. It suggests that the heating temperature and method introduced were insufficient to reduce the tensile strength to a certain level but managed to soften the blank's core. Moreover, the die heating time was the longest compared to the other. As a result, it explains why the thinning condition can be improved, but the cup's wall thickness distribution was widely scattered.

The warm sheet metal drawing performed at low heating temperatures, ranging from 100°C to 150°C, has created cups with minor improvement in thickness distribution and the thinning condition. This is because low heating temperatures were insufficient for MS and SS304 to impart enough material's ductility. Although a low heating temperature can be reached quickly to the blank's core, MS and SS304 have low thermal conductivity. Therefore, it can be said that only a few of the blank's sections have been heated to the desired temperature, and uneven temperature distribution within the blank occurs. Therefore, when the blank is driven into the die cavity by the punch, it is not uniformly deformed, and the thickness distribution is widely dispersed along the cup's wall. These results prove that warm sheet metal drawing under certain heating conditions can improve thickness distribution and thinning conditions at the punch corner.

4.2.4 Simulation

ABAQUS/CAE is used to simulate the sheet metal drawing process of the circular

cup. It started with designing a 3D model of apparatus setup consisting of punch, blank holder, die, and blank sheet, as shown in Figure 4.4. The blank is placed between the blank holder and the die. Then, the blank is pushed into the die cavity during the simulation process. After the process is finished, FEA is conducted on the thickness distribution within the cup, as shown in Figure 4.5.

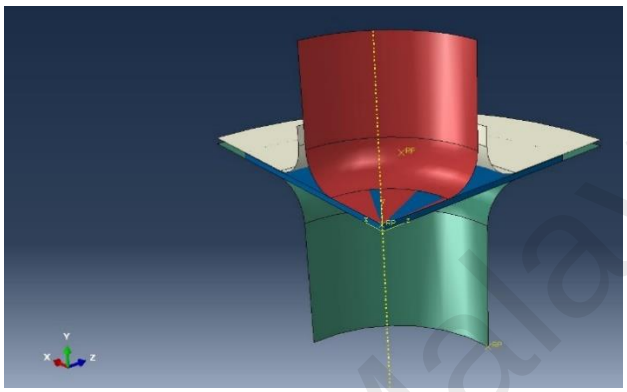

Figure 4.4: 3D model of circular sheet metal drawing tools setup

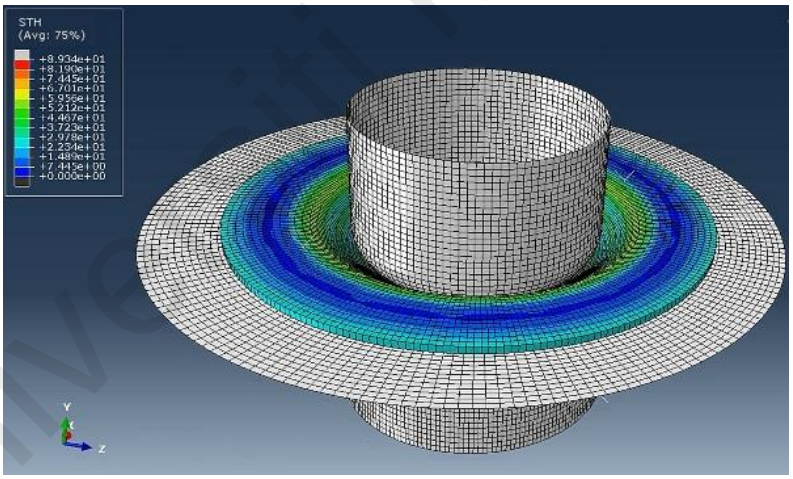

Figure 4.5: FEA on thickness distribution for the circular sheet metal drawing process

For ABAQUS thickness distribution analysis, essential parameters such as boundary condition, load, part mesh, material and section properties must be defined. ABAQUS then will predict the thickness distribution as tabulated in Appendix C. The ABAQUS thickness distribution was recorded at twenty-five (25) points along the drawn cup's cross-sectional area and focused on the punch corner area. The standard deviation and minimum

thickness for ABAQUS simulation and experimental works will be compared in Table 4.3. The detailed graph and descriptive numerical table can be referred to Appendix C.

Table 4.3: Analysis of thickness distribution in circular sheet metal drawing simulation from ABAQUS

Material	Exp	ABAQUS Simulation VS Experiment	Standard deviation (mm)	Percentage difference for standard deviation (%)	Minimum thickness (mm)	Percentage difference for minimum thickness (%)
AL6065	1	ABAQUS	0.047	2.19	0.928	3.00
		Experiment	0.049		0.901	
	2	ABAQUS	0.012	72.96	0.969	8.28
		Experiment	0.043		0.895	
	3	ABAQUS	N/A	N/A	N/A	N/A
		Experiment	N/A		N/A	
MS	4	ABAQUS	0.010	80.52	0.962	2.60
		Experiment	0.049		0.938	
	5	ABAQUS	0.012	75.28	0.971	13.22
		Experiment	0.050		0.858	
	6	ABAQUS	0.011	77.44	0.969	9.41
		Experiment	0.050		0.886	
SS304	7	ABAQUS	0.007	88.37	0.970	6.79
		Experiment	0.059		0.908	
	8	ABAQUS	0.012	85.38	0.967	5.61
		Experiment	0.084		1.024	
	9	ABAQUS	0.012	82.23	0.963	8.90
		Experiment	0.069		0.884	

From Table 4.3, ABAQUS's thickness distribution data have a lower standard deviation than the experiment as ABAQUS predicted less scattered data. However, compared to experiment, most of the data have a huge percentage difference, and Experiment 7 has the most significant standard deviation percentage difference with 88.37%. It can be caused by environmental factors such as insufficient lubrication during the experimental works. These factors make the standard deviation of the experiment thickness distribution higher than ABAQUS. Another contributing factor was that the punch speed modelled in ABAQUS was fixed. Therefore, during the experiment, the punch speed will be affected by the surroundings or the press table structure.

Experiment 1 has the lowest percentage difference of standard deviation with a value of 2.19%. ABAQUS simulation shows a smaller dispersion of thickness variation compared to experimental data. The difference happens because the mechanical properties value, such as friction in experimental runs, was not precisely modelled in the simulation program. This difference occurs due to environmental factors affecting the material's mechanical properties behaviour, such as rusting during the experiment. Furthermore, experimental conditions cannot be controlled entirely due to limits in equipment and facilities, human error, and environmental factors.

Most simulated data also indicate that thickening at the cup's wall edge was less likely to happen, which differs from experimental data. On top of that, the dispersion between simulated and experimental data is quite significant for the other comparison graph between ABAQUS simulation and experimental runs. Hence, it explains the percentage difference for standard deviation of other experimental runs exceeding 70%. ABAQUS simulation portrays a thicker minimum thickness from experimental data. However, the percentage difference for minimum thickness was less than 15%. It shows thinning conditions predicted from ABAQUS were close to the experiment thinning condition.

4.2.5 S/N Ratio and ANOVA for the circular cup

The quality characteristic in this experimental study using the Taguchi method is thickness distribution. As the results are desired to be a uniform thickness distribution, the quality characteristic is of the nominal-the-best type. The results are calculated after tabulating the results in Minitab 17 and applying the nominal-the-best S/N ratios on thickness distribution. Figure 4.6 shows the results of the main effect plot for S/N ratios, while the response table for the S/N ratio is shown in Table 4.4.

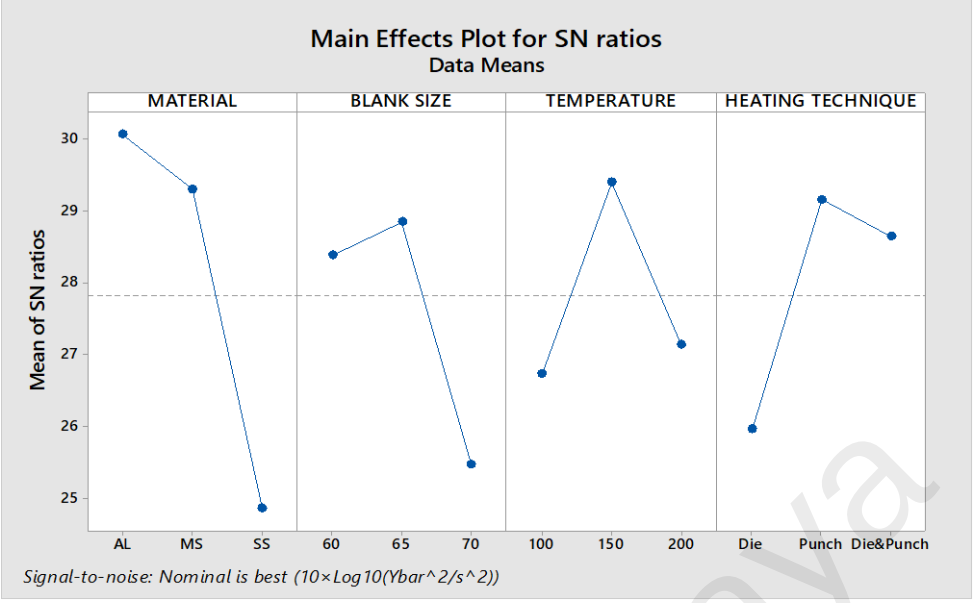

Figure 4.6: Main effect plot for S/N ratio of thickness distribution for the circular cup

Table 4.4: Response table for S/N ratio of thickness distribution for the circular cup

Level	Material	Blank size	Temperature	Heating technique
1	30.06	28.38	26.73	25.96
2	29.31	28.85	29.39	29.16
3	24.87	25.48	27.14	28.65
Delta	5.19	3.37	2.66	3.20
Rank S/N	1	2	4	3

Main effects plots determine how the factor affects the response characteristic such as S/N ratio, means, slopes, and standard deviations. Based on Figure 4.6, a nominal S/N ratio is desirable. A significant difference in the S/N ratio across factor settings implies that the factor or design parameter is essential to achieve the performance characteristic. Furthermore, the slope for each parameter in the main effect plot of the S/N ratio describes the relative relevance of the response data. The higher inclination the plot has, the higher the influence of the parameter. Figure 4.6 shows material has the steepest slope and highest delta value in Table 4.4, indicating this factor maximizes the S/N ratio for the thickness distribution of sheet metal drawn circular cups in warm temperatures.

Hence, the highest point for each factor category was selected to interpret the plot. As a result, the highest S/N ratio for material is AL6065, blank size is 65 mm, the heating temperature is 150°C, and the heating technique is punch. These combinations were the best parameter for the warm sheet metal drawing process to achieve a good thickness distribution. The details can be referred from Table 4.5**.**

Table 4.5: Optimal condition for warm sheet metal drawing of the circular cup to achieve good thickness distribution

Factor	Level Description	Level
Material	AL6065	1
Blank Size (mm)	65	2
Heating Temperature (°C)	150	2
Heating Technique	Punch	2

From the ANOVA analysis, the sum of squares due to the variation from the average S/N ratio for the *y*th factor, SS_y can be calculated. Therefore, the contribution of process parameters on the warm sheet metal drawing process in terms of percentage can be obtained as presented in Table 4.6.

Table 4.6: Contribution of process parameters on warm sheet metal drawing process to achieve good thickness distribution of the circular cup

Process Parameter	Sum of Square, *SSy*	Percentage of Contribution (%)
Material	0.3630	34.52
Blank Size (mm)	0.2371	22.54
Heating Temperature (°C)	0.2179	20.72
Heating Technique	0.2337	22.22

The ANOVA results indicate the degrees of importance of each process parameter, which are material, blank size, heating temperature, and heating technique that affect the circular cup's thickness in warm sheet metal drawing. Material has the greatest influence (34.52%) on the thickness distribution of the sheet metal drawn circular cup, followed by blank size (22.54%), heating technique (22.22%) and heating temperature (20.72%).

4.2.6 Confirmation test for circular cup

From the optimum condition obtained from Table 4.5, a confirmation test has been conducted. The outcome can be seen in Figure 4.7 shown below.

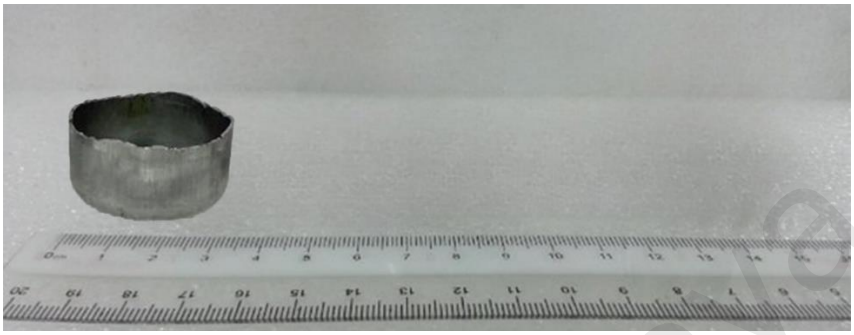

Figure 4.7: 65 mm AL6065 circular cup drawn at 150°C heated punch

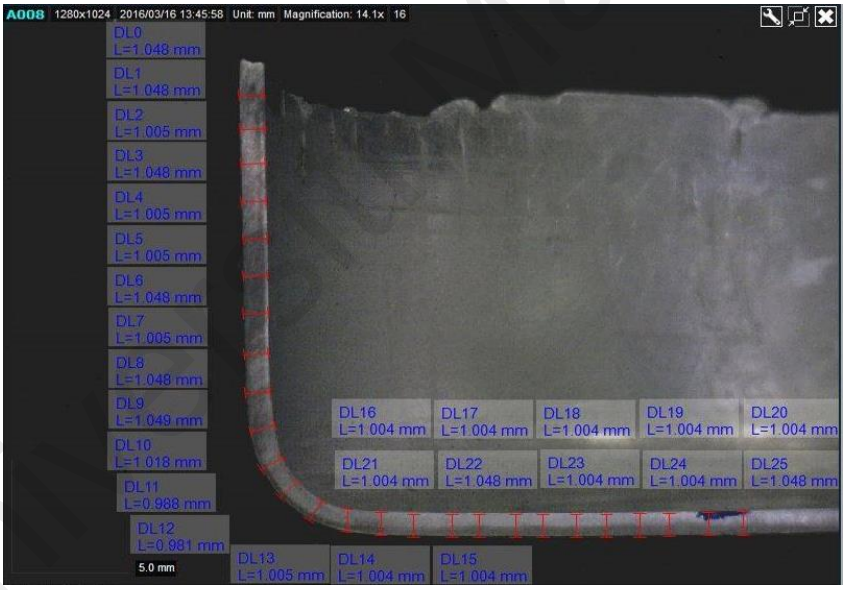

Figure 4.8: Thickness distribution of 65 mm AL6065 circular cup drawn at 150°C heated punch

From the outcome of both figures, the optimization of cup's wall thickness has been achieved. This is due to the cup wall minimum thickness and the thickness distribution has been improved in warm condition compared to room temperature condition.

4.3 Square sheet metal drawn cup

4.3.1 Limiting drawing ratio (LDR) for the square cup

Each experiment's outcome is observed and documented. Appendix D illustrates the square cups formed in the room and warm temperatures. Table 4.7 shows the LDR for AL6065, MS, and SS304 in the room and warm sheet metal drawing.

AL6065, MS, and SS304 have a maximum LDR of 1.38, 1.54, and 1.69 in warm sheet metal drawing. Meanwhile, the maximum LDR for AL6065 is 1.38, while mild and SS304 is 1.69 at room temperature sheet metal drawing. According to

Table 4.7, tearing defects occurred in 50 mm and 55 mm AL6065 blanks during room and warm sheet metal drawing, but MS blanks only happened during warm sheet metal drawing.

Table 4.7: LDR for AL6065, MS, and SS304 in the room and warm sheet metal drawing for the square cup

Exp no.	Material	Blank Size (mm)	Temperature (°C)	Heating Technique	Results	LDR
1	AL6065	45	100	Die	Successful	1.38
			Room temp	N/A	Successful	1.38
2		50	150	Punch	Failed	-
			Room temp	N/A	Failed	-
3		55	200	Die & Punch	Failed	-
			Room temp	N/A	Failed	-
4	MS	45	150	Die & Punch	Successful	1.38
			Room temp	N/A	Successful	1.38
5		50	200	Die	Successful	1.54
			Room temp	N/A	Successful	1.54
6		55	100	Punch	Failed	-
			Room temp	N/A	Successful	1.69
7	SS304	45	200	Punch	Successful	1.38
			Room temp	N/A	Successful	1.38
8		50	100	Die & Punch	Successful	1.54
			Room temp	N/A	Successful	1.54
9		55	150	Die	Successful	1.69
			Room temp	N/A	Successful	1.69

AL6065 is more prone to thinning at the punch corner region than MS or SS304 because of its lower tensile strength. Additionally, the stress concentration is greater at the square punch corner region than at the circular punch corner region, resulting in fractures in AL6065 and MS blanks.

For square warm sheet metal drawing, the heater is inserted into the die shoe and seems to have slower heat conduction to the blank. As a result, the heating procedure at 150°C and 200°C took more than two hours to achieve the necessary temperature on the blank. There is a thermal difference between the flange area and the blank centre during this heat conduction procedure.

However, when the blank is forced into the die cavity by the hot punch, the strength of the blank at its centre is reduced. The large concentration of stress at the punch corner contributes to the flow stress, which finally exceeds the material strength. Then, this area loses a significant amount of thickness, resulting in cup wall thinning. The thinning develops as the punch travels deeper to drive the blank into the die cavity, causing the tearing defect.

4.3.2 Average square cup height

Figure 4.9 compares the average square cup's height according to the blank sizes for AL6065, MS, and SS304 in the room and warm sheet metal drawing. The average square cup height for AL6065, MS and SS304 in the room and warm sheet metal drawing are recorded in Appendix E.

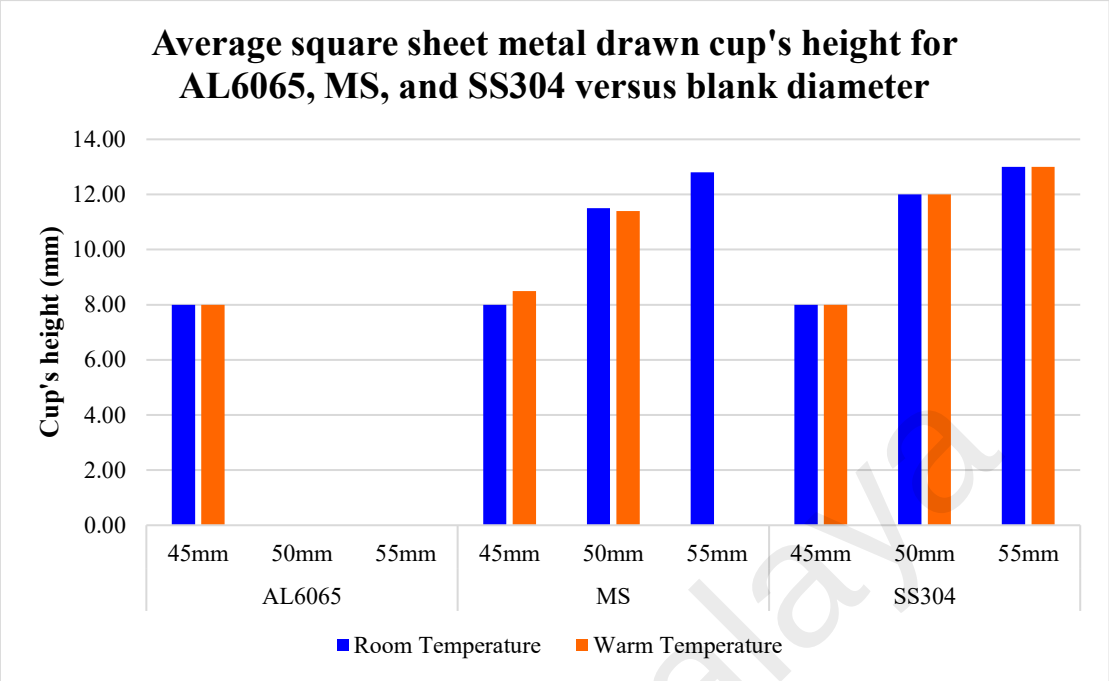

Figure 4.9: Average square sheet metal drawn cup's height for AL6065, MS, and SS304 versus blank diameter

Most of the square cups drawn from the room and warm sheet metal drawing have almost the same heights, except for the MS blanks of 45 mm and 50 mm. For 45 mm blank size, the average cup's height obtained from warm sheet metal drawing is higher than the room temperature sheet metal drawing, while it happened oppositely for 55 mm blank size. However, these average square cup height differences are considered small, between 0.03 mm and 0.50 mm. Therefore, the effect of temperature on the average height of a square cup is negligible.

4.3.3 Thickness distribution for the square cup

For square sheet metal drawing, the thickness is often homogeneous at the punch's bottom face, minimal at the punch nose radius and vertical surface, and thicker at the flange area. In this study, the thickness distributions were measured starting from the edge of the cup wall to the bottom centre, as shown in Figure 4.10. Before measuring the thickness distribution, the sheet metal drawn circular cup is dissected, and the extra burr removed. It was measured using a Dino-Lite Premier AM7013MZT4 digital microscope, and twenty-five (25) points were recorded along the drawn cup's cross-sectional area. The thickness distribution of the drawn cup in the room and warm sheet metal drawing was presented in Figure 4.11. The tabulated data can be referred to Appendix E.

Figure 4.10: Illustration of measuring position along the square cup profile

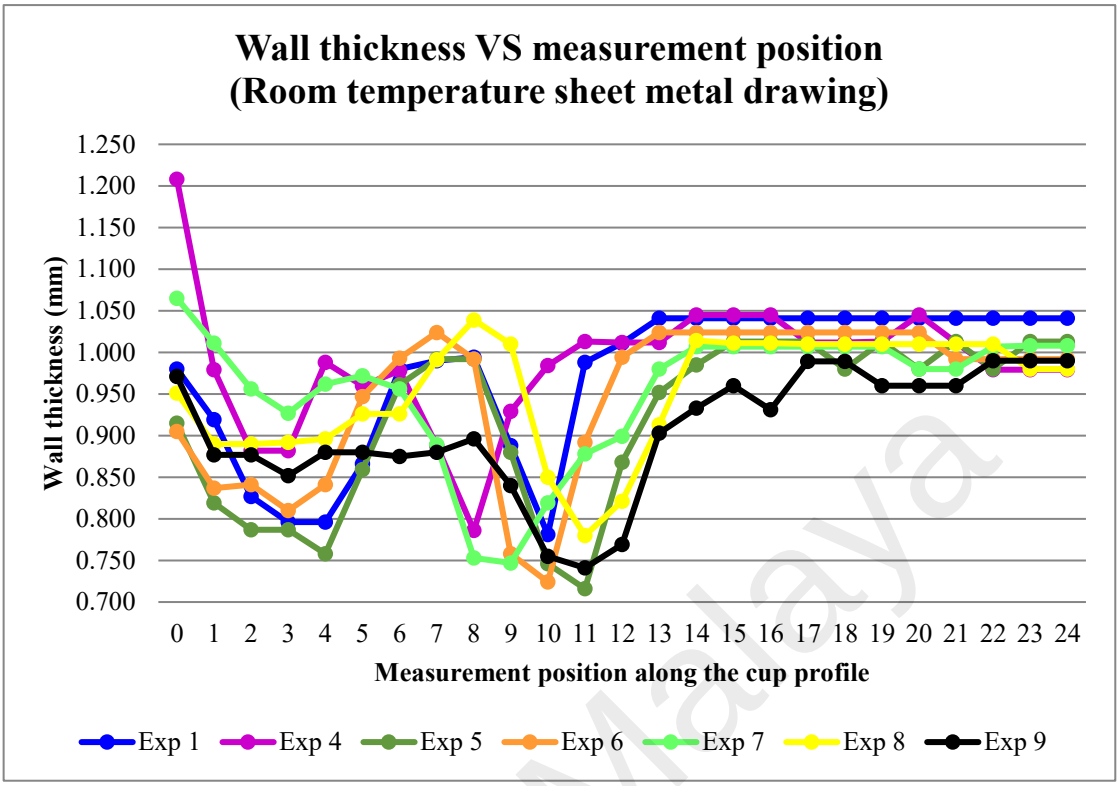

(a)

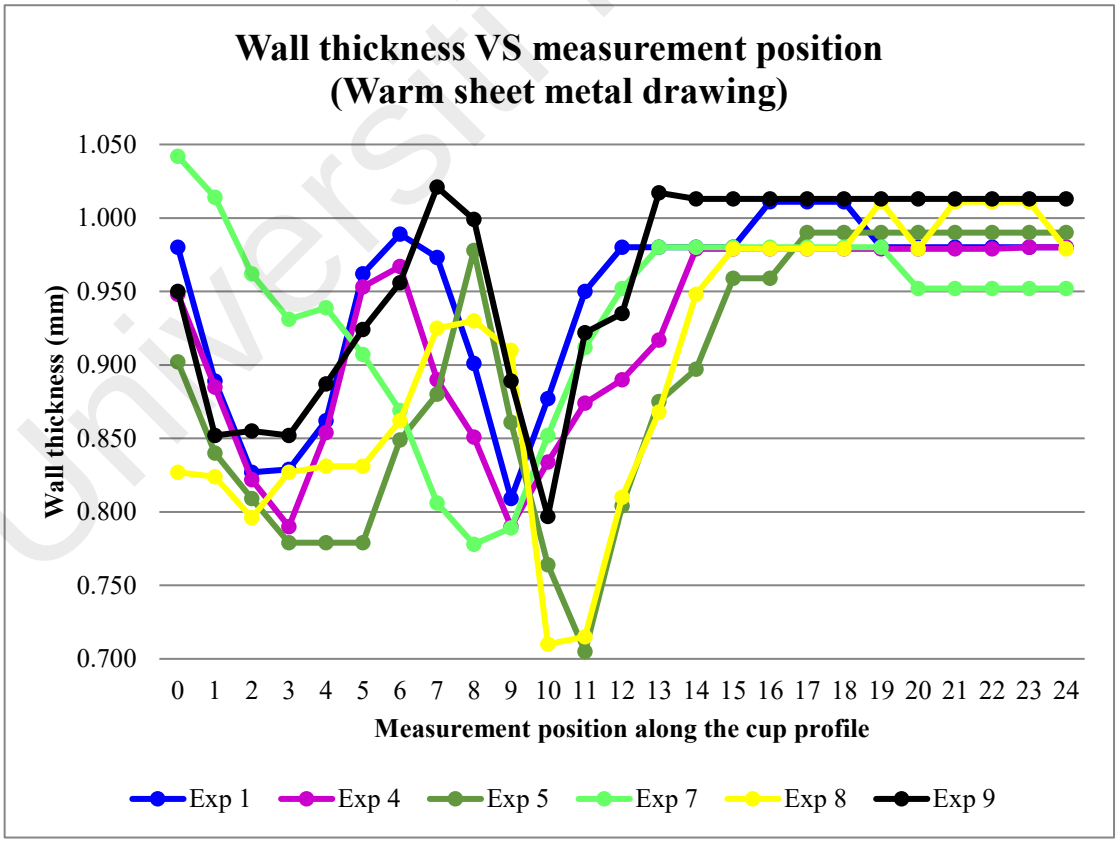

(b)

Figure 4.11: Thickness distribution along the square cup profile in the sheet metal drawing process conducted at (a) room temperature and (b) warm temperature

The square cups used in Experiments 2 and 3 could not be deformed appropriately for room temperature sheet metal drawing. Simultaneously, square cups from Experiments 2, 3, and 6 failed to deform due to tearing during warm sheet metal drawing. However, Figure 4.11(a) and Figure 4.11(b) demonstrated uneven thickening at the flange, thinning at the vertical surface and punch radius, and uniform thickness at the punch's bottom face. There was insufficient stress to cause permanent deformation of the square cup's bottom face region, resulting in a uniform and almost identical to the initial blank thickness. In general, warm sheet metal drawing enhanced the thickness distribution. Additionally, while sheet metal drawing at room temperature, the drawn cup suffers significantly more thinning at the punch corner than warm sheet metal drawing.

Due to the geometrical factor, the cup's punch corner thins due to the large concentration of stress in this location. As a result, the material in this region will first bend around the die radius and then unbend when tensile stress is applied to the die wall. Following that, it bends in the other way around the punch corner. As a result, this area is vulnerable to serious thinning, which results in tearing flaws. It was similar to the outcome of Kardan et al., (2018) work.

A lack of material flow produces the thickness variation into the die cavity, which is particularly noticeable while sheet metal was drawn at room temperature. On the other hand, thickening occurs in the flange due to compressive stress and circumferential shrinkage. As a result, minor wrinkling is unavoidable in this region, causing the thickening around the top edge of the cup’s wall. Further analysis will compare the standard deviation and minimum thickness for the cup drawn in the room and warm temperature, as shown in Table 4.8. The detailed graph and descriptive numerical table can be referred to Appendix E.

Table 4.8: Analysis of thickness distribution in square sheet metal drawing experiment

Material	Exp	Temperature and heating technique	Standard deviation (mm)	Percentage difference for standard deviation (%)	Minimum thickness (mm)	Percentage difference for minimum thickness (%)
AL6065	1	RT	0.091	38.49	0.781	3.52
		100°C; Die	0.062		0.809	
	2	RT	N/A	N/A	N/A	N/A
		150°C; Punch	N/A		N/A	
	3	RT	N/A	N/A	N/A	N/A
		200°C; Die & Punch	N/A		N/A	
MS	4	RT	0.077	14.35	0.786	0.51
		150°C; Die & Punch	0.067		0.790	
	5	RT	0.100	8.31	0.716	1.55
		200°C; Die	0.092		0.705	
	6	RT	N/A	N/A	N/A	N/A
		100°C; Punch	N/A		N/A	
SS304	7	RT	0.081	18.50	0.747	4.07
		200°C; Punch	0.068		0.778	
	8	RT	0.071	27.63	0.780	9.40
		100°C; Die & Punch	0.093		0.710	
	9	RT	0.074	2.19	0.741	7.28
		150°C; Die	0.069		0.797	

According to Table 4.8, most warm sheet metal drawing experiments result in a smaller standard deviation for the cup's wall thickness than room temperature sheet metal drawing. It illustrates that the thickness variation in the warm sheet metal drawing is often closer to the mean and less dispersed. Except for Experiment 8, all drawn cups from warm sheet metal drawing exhibit a more uniform thickness distribution than those drawn from room temperature sheet metal drawing.

However, the standard deviation difference for Experiment 8 in the room and warm sheet metal drawing is 27.63% and considered as high. It demonstrates that the improvement was not accomplished even after the temperature gradient was implemented. Experiment 8 required nearly six hours to heat the blank to the desired temperature. Even after repeating the method twice more, the heating process took enormous time. As this happens, a slight heat difference between the flange area and the blank center exists during this heat conduction process. Thus, as the blank is forced into the die cavity by the hot punch, the elongation of the cup's wall is not uniform, contributing to more scattered thickness variation.

There were also chances of diffusion taking place across the sheet metals' grain boundaries after undergoing a long heating process. It will cause a larger grain size that will disrupt the sheet metal's strength and contribute to the highly dispersed thickness variation of a square sheet metal drawn cup. However, this assumption needs to undergo further analysis to verify.

The heating temperature and procedures enhance the wall thickness distribution along the cup's profile for the remaining experimental runs. The most significant standard deviation improvement is 38.49% in Experiment 1 when a heating temperature of 100°C is applied to 45 mm AL6065 blanks using the die heating technique. In contrast, Experiment 9 has 2.19%, and Experiment 5 has an 8.31% standard deviation difference for room and warm sheet metal drawing. Both were deemed minor standard deviation improvements that can be further improved.

Meanwhile, all warm sheet metal drawings except Experiments 5 and 8 have improved the minimum thickness that often occurs in the punch corner area. However, the percentage differences between room and heated sheet metal drawing were 1.55%

and 9.40%, respectively, which were deemed insignificant. Additionally, in Experiment 4, the square cup's percentage difference for a minimum thickness of 0.51% improved slightly. It indicates that while heating conditions increase the thickness distribution, the improvement is minor and almost insignificant.

Experiment 9 shows the greatest improvement in minimum thickness, with the percentage difference between room and warm sheet metal drawing increasing by 7.28%. However, it is still considered a minor improvement as the expected percentage difference is more than 15%. The minimum thickness can be improved by having a deeper die cavity, extended punch, and bigger die corner radius. The smaller the die radius, the greater the force on the blank, resulting in thinner wall thickness. On the other hand, the square cups are not totally deformed due to the punch's height limitation. As a result, the material cannot be entirely drawn into the die cavity, resulting in incomplete material flow. Hence, the cup's thickness is unevenly distributed.

The warm sheet metal drawing performed at low heating temperatures, ranging from 100°C to 150°C, has created cups with minor improvement in thickness distribution and the thinning condition. This is because low heating temperatures were insufficient for MS and SS304 to impart enough material’s ductility. Although a low heating temperature can be reached quickly to the blank’s core, MS and SS304 have low thermal conductivity. Therefore, it can be said that only a few of the blank sections have been heated to the desired temperature, and uneven temperature distribution within the blank occurs. Therefore, when the blank is driven into the die cavity by the punch, it is not uniformly deformed, and the thickness distribution is widely dispersed along the cup’s wall. These results prove that warm sheet metal drawing under certain heating conditions can improve thickness distribution and thinning conditions at the punch corner.

4.3.4 Simulation

ABAQUS/CAE is used to simulate the sheet metal drawing process of the square cup. It began with the creation of a three-dimensional model of cup symmetry. This 3D model depicts the arrangement of the tools' set, which includes the punch, blank holder, die, and blank sheet, as illustrated in Figure 4.12. The blank is inserted between the blank holder and the die before the simulation. The blank is then pushed into the die cavity during the simulation procedure. After the process is finished, FEA is conducted on the thickness distribution within the cup, as shown in Figure 4.13.

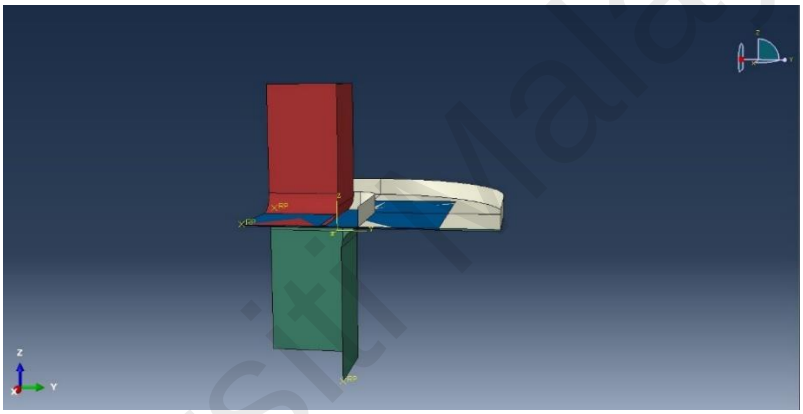

Figure 4.12: 3D model of square sheet metal drawing tool setup

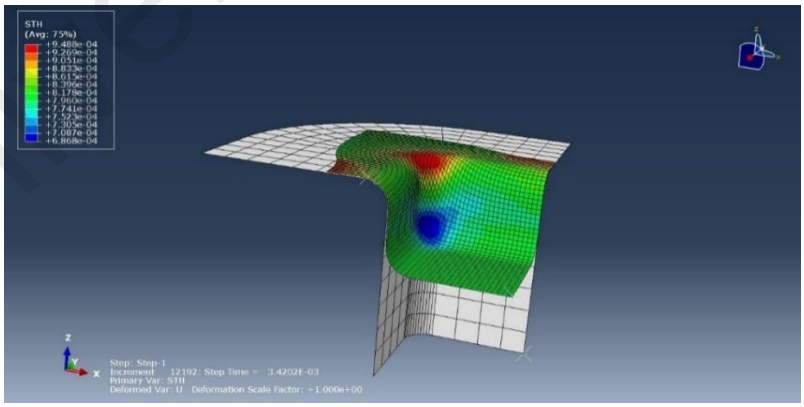

Figure 4.13: FEA on thickness distribution for circular sheet metal drawing process

For ABAQUS thickness distribution analysis, essential parameters such as boundary condition, load, part mesh, material, and section properties must be defined. ABAQUS then will predict the thickness distribution as tabulated in Appendix F. The ABAQUS

thickness distribution was recorded at twenty-five (25) points along the drawn cup's cross-sectional area and focused on the punch corner area. The standard deviation and minimum thickness for ABAQUS simulation and experimental works will be compared in Table 4.9. The detailed graph and descriptive numerical table can be referred to Appendix F.

Table 4.9: Analysis of thickness distribution in square sheet metal drawing simulation from ABAQUS

Material	Exp	ABAQUS Simulation VS Experiment	Standard deviation (mm)	Percentage difference for standard deviation (%)	Minimum thickness (mm)	Percentage difference for minimum thickness (%)
AL6065	1	ABAQUS	0.047	48.07	0.835	6.94
		Experiment	0.091		0.781	
	2	ABAQUS	N/A	N/A	N/A	N/A
		Experiment	N/A		N/A	
	3	ABAQUS	N/A	N/A	N/A	N/A
		Experiment	N/A		N/A	
MS	4	ABAQUS	0.026	66.06	0.846	7.63
		Experiment	0.077		0.786	
	5	ABAQUS	0.017	82.80	0.828	15.64
		Experiment	0.100		0.716	
	6	ABAQUS	0.009	90.12	0.872	20.50
		Experiment	0.094		0.724	
SS304	7	ABAQUS	0.009	88.39	0.881	17.99
		Experiment	0.081		0.747	
	8	ABAQUS	0.011	83.86	0.867	11.18
		Experiment	0.071		0.780	
	9	ABAQUS	0.011	84.86	0.868	17.17
		Experiment	0.074		0.741	

From Table 4.9, ABAQUS's thickness distribution data have a lower standard deviation than the experiment as ABAQUS predicted less scattered data based on the input parameters. However, compared to experimental works, most of the data have a huge percentage difference, and Experiment 6 has the most significant standard deviation percentage difference with 90.12%. The difference is caused by environmental factors such as insufficient lubrication during the experimental works. These factors make the standard deviation of the experiment thickness distribution higher than ABAQUS.

Another factor contributing to this huge difference was that the punch speed modelled in ABAQUS was fixed. Therefore, the punch speed will be affected by the surroundings or the press table structure during the experiment.

Experiment 1 has the lowest percentage difference of standard deviation with a value of 48.07%. ABAQUS simulation portrays smaller dispersion of thickness variation compared to experimental data. The difference was due to the mechanical properties value, such as friction in experimental runs was not precisely modelled in the simulation program. This difference happened due to environmental factors causing blank rust during the experiment. Furthermore, experimental conditions cannot be controlled entirely due to limits in equipment and facilities, human error, and environmental factors.

Most simulated data also indicate that thickening at the cup's wall edge was less likely to happen, which differs from experimental data. On top of that, the dispersion between simulated and experimental data is quite significant for the other comparison graph between ABAQUS simulation and experimental runs. Hence, it explains the percentage difference for standard deviation of other experimental runs exceeding 70%. ABAQUS simulation portrays a thicker minimum thickness from experimental data.

However, the percentage difference between ABAQUS simulation and experimental data for minimal thickness was about 20%. Consequently, it shows thinning conditions predicted from ABAQUS were close to the experiment thinning condition.

4.3.5 S/N Ratio and ANOVA for the square cup

The quality characteristic in this experimental study using the Taguchi method is thickness distribution. As the results are desired to be a uniform thickness distribution, the

quality characteristic is of the nominal-the-best type. The results are calculated after tabulating the result data in Minitab 17 and applying the nominal-the-best S/N ratios on thickness distribution. Figure 4.14 shows the results of main effect plot for S/N ratios, while the response table for the S/N ratio is shown in Table 4.10.

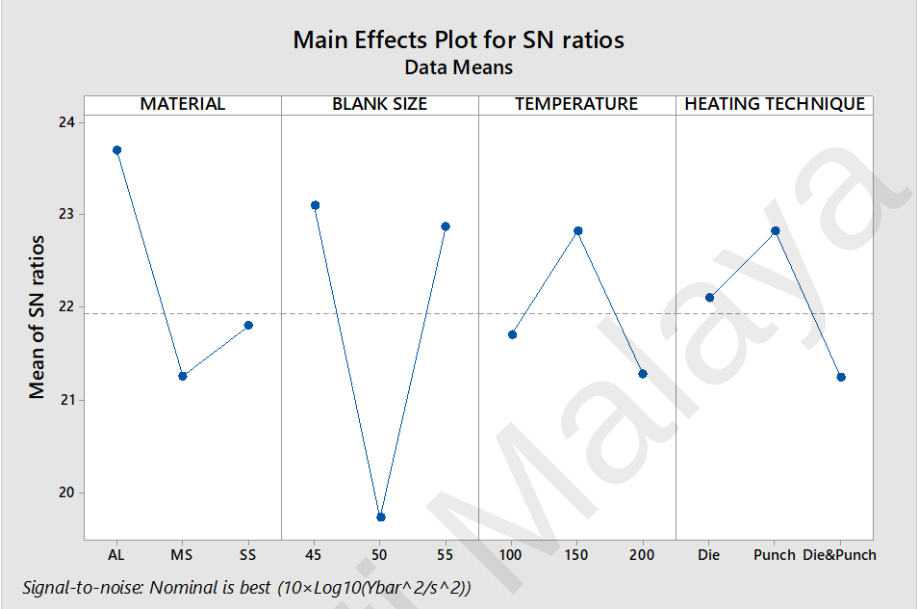

Figure 4.14: Main effect plot for S/N ratio of thickness distribution for the square cup

Table 4.10: Response table for S/N ratio of thickness distribution for the square cup

Level	Material	Blank size	Temperature	Heating technique
1	23.70	23.10	21.71	22.10
2	21.26	19.73	22.82	22.82
3	21.80	22.87	21.28	21.24
Delta	2.44	3.37	1.54	1.58
Rank S/N	2	1	4	3

The factor's influence on response characteristics such as the S/N ratio, means, slopes, and standard deviations is determined via main effects plots. Figure 4.14 shows that a nominal S/N ratio is preferable. A significant difference in the S/N ratio across factor settings implies that the factor or design parameter is essential to achieve the performance characteristic. Furthermore, the slope for each parameter in the main effect plot of the

S/N ratio describes the relative relevance of the response data. The higher inclination the plot has, the higher the influence of the parameter. Figure 4.14 shows that blank size has the greatest slope and highest delta value in Table 4.10. This element maximizes the S/N ratio for the thickness distribution of sheet metal drawn square cups at warm temperatures.

Hence, the highest point for each factor category was selected to interpret the plot. As a result, the highest S/N ratio for material is AL6065, blank size is 45 mm, the heating temperature is 150°C, and the heating technique is punch. These combinations were the best parameter for the warm sheet metal drawing process to achieve a good thickness distribution. The details can be referred from Table 4.11.

Table 4.11: Optimal condition for warm sheet metal drawing of the square cup to achieve good thickness distribution

Factor	Level Description	Level
Material	AL6065	1
Blank Size (mm)	45	1
Heating Temperature (°C)	150	2
Heating Technique	Punch	2

From the ANOVA analysis, the sum of squares due to the variation from the average S/N ratio for the yth factor, SS_y can be calculated. Therefore, the contribution of process parameters on the warm sheet metal drawing process in terms of percentage can be obtained as presented in Table 4.12. The blank size has the highest percentage of contribution, followed by material, heating technique, and heating temperature.

Table 4.12: Contribution of process parameters on warm sheet metal drawing process to achieve good thickness distribution of the square cup

Process Parameter	Sum of Square, SSy	Percentage of Contribution (%)
Material	0.57047	33.17
Blank Size (mm)	0.58068	33.76
Heating Temperature (°C)	0.00048	0.03
Heating Technique	0.56818	33.04

The ANOVA results indicate the degrees of importance of each process parameter, which are material, blank size, heating temperature, and heating technique that affect the square cup's thickness in warm sheet metal drawing. Blank size has the greatest influence (33.76%) on the thickness distribution of the sheet metal drawn square cup, followed by material (33.17%), heating technique (33.04%), and heating temperature (0.03%).

4.3.6 Confirmation test for square cup

From the optimum condition obtained from Table 4.11, a confirmation test has been conducted. The outcome can be seen in Figure 4.7 shown below.

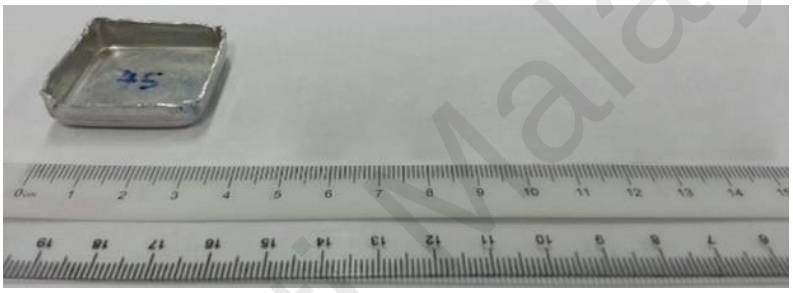

Figure 4.15: 45 mm AL6065 circular cup drawn at 150°C heated punch

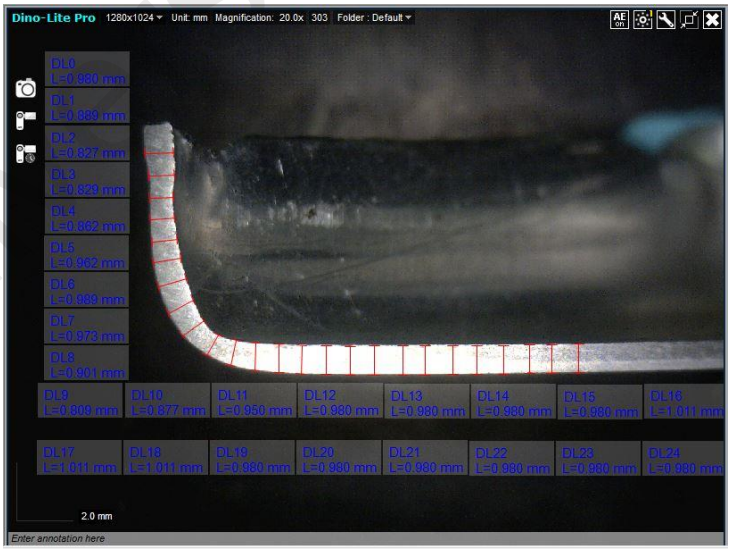

Figure 4.16: Thickness distribution of 45 mm AL6065 circular cup drawn at 150°C heated punch

From both figures, the optimization has been achieved as the cup's wall minimum thickness and thickness distribution has been improved in warm condition.

CHAPTER 5: CONCLUSION

5.1 Introduction

The primary goal of this study is to examine the tooling temperature effects towards circular and square sheet metal drawing. Moreover, an evaluation of the effect of different process parameters on the warm sheet metal drawing is made. Then, FEA simulation was conducted to predict the thickness distribution along the cup wall and compared to experimental data to examine the cup's drawability. The conclusions were deduced based on the research objectives presented in this chapter.

5.2 Conclusion

5.2.1 The effect of tooling temperature on circular and square sheet metal drawing

In this study, there were effects of tooling temperature on circular and square sheet metal drawing. For circular sheet metal drawing, the results of LDR show that AL6065 with 70 mm blank size cannot be successfully formed when the punch is heated to 200°C. There is an upper limit for heating temperature. Above this upper limit, the strength of the material is lost. On top of that, the heating time to achieve the desired temperature was quite long and varied for each run. The high-stress concentration at the punch corner, fracture and tearing defects in the AL6065 cup.

On the other hand, the tooling temperature affects LDR for square warm sheet metal drawing. AL6065 has the lowest LDR value, 1.38, followed by MS with 1.54 and SS304 with 1.69. Tearing defect happened for 50 mm and 55 mm of AL6065 blank at room and warm sheet metal drawing, while only 55 mm of MS blank at warm sheet metal drawing. Due to the slower heat conduction rate to heat the blank, the heating process took a long time to be fulfilled. As a result, the heat difference between the flange and the blank centre area existed, causing a decrement of strength at the blank centre. In addition, the

high-stress concentration at the punch corner contributes to the flow stress and eventually makes it greater than the material strength. Then, this region loses a substantial thickness and eventually tears the cup's wall.

For thickness distribution, warm tooling temperature has positive impacts. The results of thickness distribution in both circular and square sheet metal drawing show that thickness is more uniformly distributed along the cup's wall under certain heating conditions, and maximum thinning at the punch corner is reduced compared to sheet metal drawing at room temperature. However, when a low heating temperature is given to both circular and square sheet metal drawing, a slight improvement in thickness distribution or thinning occurs, indicating a lower heating temperature limit exists. As the low heating temperature took a varied heating duration, uneven temperature distribution occurred. It makes the residual stresses within the blank cannot be overcome and cause the uneven deformation of the blank.

In contrast, warm tooling temperature has a minor impact on average circular and square cup height. The circular cup's average height is around 1.00 mm, while the square cup's average height improvement ranges between 0.03 mm and 0.50 mm. Thus, there is no significant improvement towards the average cup's height, and the effect of tooling temperature is negligible.

5.2.2 The effect of different process parameters on warm sheet metal drawing

For the effect of different process parameters on circular warm sheet metal drawing, ANOVA was utilised. It shows that the material has the greatest influence (34.52%) on the thickness of the circular cup, followed by blank size (22.54%), heating technique (22.22%) and heating temperature (20.72%). The main effect plot of S/N ratio shows that the combination of AL6065 with blank size 65 mm, the heating temperature of 150°C and the punch heating technique is optimal to obtain uniform thickness

distribution of the circular cup.

For square warm sheet metal drawing, ANOVA results show that blank size has the greatest influence (33.76%) on the thickness distribution of the sheet metal drawn square cup, followed by material (33.17%), heating technique (33.04%) and heating temperature (0.03%). The main effect plot of S/N ratio shows that the combination of AL6065 with blank size 45 mm, the heating temperature of 150°C and the punch heating technique is optimal to obtain uniform thickness distribution of the square cup.

5.2.3 Comparison of the thickness distribution within the drawn cup between experiment and finite element analysis

In circular and square sheet metal drawing, FEA simulation from ABAQUS predicts thickening at the flange, thinning at the punch radius, and consistent thickness at the punch's bottom face, similar to experimental outcomes. However, a significant standard deviation difference exists between the simulation and experimental results due to assumptions and uncontrollable conditions. For example, the mechanical and physical properties of the material used during the experiment can be altered due to environmental factors such as rusting. Moreover, the friction coefficient modelled in FEA may not precisely mimic the actual experiment condition that was highly influenced by the lubrication factor.

Nevertheless, for thinning conditions, close predictions were made by ABAQUS when compared to experimental outcomes. The circular cup's minimum thickness difference was 15%, while the square cup’s was 20%. Insufficient die throat tolerance will cause the square cup’s minimum thickness difference to be higher than the circular cup. It concludes that thinning conditions predicted from ABAQUS were close to the experiment thinning condition.

5.3 Recommendations

Several suggestions and recommendations can be drawn out to improve future works. The current square die set has an insufficient die and punch corner radius and the die's cavity length from the tooling setup aspect. A bigger die and punch corner radius allow easier material flow and reduce the stress exerted on the blank. Moreover, a deeper die cavity can enhance the probability of having a good and fully deformed cup. The method of heating the tooling setup should be improved by placing the heater directly on the blank holder or the blank to reduce the heating time.

REFERENCES

Abdul Ghafar, A., Abdullah, A. B., & Mahmood, J. I. (2021). Experimental and numerical prediction on square cup punch–die misalignment during the deep drawing process. *International Journal of Advanced Manufacturing Technology*, *113*(1–2).

Ambrogio, G., Filice, L., Palumbo, G., & Pinto, S. (2005). Prediction of formability extension in deep drawing when superimposing a thermal gradient. *Journal of Materials Processing Technology*, *162–163*(SPEC. ISS.), 454–460.

Antony, J. (2014). Design of Experiments for Engineers and Scientists: Second Edition. In *Design of Experiments for Engineers and Scientists: Second Edition* (2nd Edition).

Banabic, D. (2010). Sheet Metal Forming Processes: Constitutive Modelling and Numerical Simulation. In *Springer-Verlag Berlin*.

Behrens, G., Ruhe, M., Tetzel, H., & Vollertsen, F. (2015). Effect of tool geometry variations on the punch force in micro deep drawing of rectangular components. *Production Engineering*, *9*(2), 195–201.

Bong, H. J., Barlat, F., Ahn, D. C., Kim, H. Y., & Lee, M. G. (2013). Formability of austenitic and ferritic stainless steels at warm forming temperature. *International Journal of Mechanical Sciences*, *75*, 94–109.

Chen, F.-K., Huang, T.-B., & Chang, C.-K. (2003). Deep drawing of square cups with magnesium alloy AZ31 sheets. *International Journal of Machine Tools and Manufacture*, *43*(15), 1553–1559.

Chen, X., & Sowerby, R. (1996). Blank development and the prediction of earing in cup drawing. *International Journal of Mechanical Sciences*, *38*(5), 509–516. https://doi.org/10.1016/0020-7403(95)00068-2

Colgan, M., & Monaghan, J. (2003). Deep drawing process: Analysis and experiment. *Journal of Materials Processing Technology*, *132*(1–3), 35–41.

Dahaam Younis, A. (2013). The effect of using Non-Uniform Blank Holder Force in Deep Drawing process on the thickness distribution along the cup_ENG. *AL-Rafdain Engineering Journal (AREJ)*, *21*(2).

Davis, J. R. (Joseph R. . (2004). *Tensile testing* (2nd ed.). ASM International.

Desu, R. K., Singh, S. K., & Gupta, A. K. (2015). Comparative study of warm and hydromechanical deep drawing for low-carbon steel. *The International Journal of Advanced Manufacturing Technology*, 11.

Dwivedi, R., & Agnihotri, G. (2015). Numerical Simulation and Experimental Analysis on the Deep Drawing of Cylindrical Cups. *Transactions of the Indian Institute of Metals*, *68*(1), 31–34.

El-Morsy, A.-W., & Manabe, K.-I. (2006). Finite element analysis of magnesium AZ31 alloy sheet in warm deep-drawing process considering heat transfer effect. *Materials Letters*, *60*(15), 1866–1870.

El Sherbiny, M., Zein, H., Abd-Rabou, M., & El shazly, M. (2014). Thinning and residual stresses of sheet metal in the deep drawing process. *Materials and Design*, *55*, 869–879.

Emmens, W. C. (2011). Formability: A Review of Parameters and Processes that Control, Limit or Enhance the Formability of Sheet Metal. In *Springer Heidelberg Dordrecht* (Vol. 7).

Ethiraj, N., & Senthil Kumar, V. S. (2012). Finite element method based simulation on warm deep drawing of AISI 304 steel circular cups. *Procedia Engineering*, *38*, 1836–1851.

Gao, E. zhi, Li, H. wei, Kou, H. chao, Chang, H., Li, J. shan, & Zhou, L. (2009). Influences of material parameters on deep drawing of thin-walled hemispheric surface part. *Transactions of Nonferrous Metals Society of China (English Edition)*, *19*(2).

Gavas, M., & Izciler, M. (2007). Effect of blank holder gap on deep drawing of square cups. *Materials and Design*, *28*(5), 1641–1646.

Ghaffari Tari, D., Worswick, M. J., & Winkler, S. (2013). Experimental studies of deep drawing of AZ31B magnesium alloy sheet under various thermal conditions. *Journal of Materials Processing Technology*, *213*(8), 1337–1347.

Goud, R. R., Prasad, K. E., & Singh, S. K. (2014). Formability Limit Diagrams of Extra-deep-drawing Steel at Elevated Temperatures. *Procedia Materials Science*, *6*(Icmpc), 123–128.

Groover, M. P. (2013). Fundamentals of Modern Manufacturing Material, Processes, and Systems, 5th Edition. In *Journal of Chemical Information and Modeling*.

Hassan, M., Hezam, L., El-Sebaie, M., & Purbolaksono, J. (2014). Deep drawing characteristics of square cups through conical dies. *Procedia Engineering*, *81*(October), 873–880.

Heinz Tschaetsch. (2004). Metal Forming Practise. In *Chemistry & …*. Vieweg Verlag,Wiesbaden 2005.

Herrmann, J., & Merklein, M. (2018). Improvement of deep drawability of ultra-fine grained 6000 series aluminum alloy by tailored heat treatment. *Procedia Manufacturing*, *15*, 976–983.

Ivana Suchy. (2006). Handbook of Die Design. In *Chemistry & …* (2nd Editio). McGraw-Hill.

Kardan, M., Parvizi, A., & Askari, A. (2018). Experimental and Finite Element Results for Optimization of Punch Force and Thickness Distribution in Deep Drawing Process. *Arabian Journal for Science and Engineering*, *43*(3), 1165–1175.

Kotkunde, N., Badrish, A., Morchhale, A., Takalkar, P., & Singh, S. K. (2020). Warm deep drawing behavior of Inconel 625 alloy using constitutive modelling and anisotropic yield criteria. *International Journal of Material Forming*, *13*(3), 355–369.

Kou, H., Qin, L., El-Aty, A. A., Liu, Y., Zhu, X., & Tao, J. (2021). Effect of temperature on the deep drawing forming performance of Ti/Al laminates: experimental investigation and finite element analysis. *International Journal of Advanced Manufacturing Technology*, *114*(9–10), 2617–2632.

Krupal S., Darshan, B., Twinkle, P., Dhruv, P. and Bharat, D. (2014). Influence of the Process Parameters in Deep Drawing. *International Journal of Emerging Research in Management &Technology*, *3*(11), 16–22.

Kuo, C. C., Lin, B. T., & Wang, W. T. (2019). Optimization of microridge punch design for deep drawing process by using the fuzzy Taguchi method. *International Journal of Advanced Manufacturing Technology*, *103*(1–4), 177–186.

Laurent, H., Coër, J., Manach, P. Y., Oliveira, M. C., & Menezes, L. F. (2015). Experimental and numerical studies on the warm deep drawing of an Al–Mg alloy. *International Journal of Mechanical Sciences*, *93*, 59–72.

Manabe, K. I., Soeda, K., & Shibata, A. (2021). Effects of variable punch speed and blank holder force in warm superplastic deep drawing process. *Metals*, *11*(3), 1–16.

Manna, M., & Mirzai, M. A. (2019). Investigating the operational parameters in the warm deep drawing process using the experimental method. *Journal of Computational and Theoretical Nanoscience*, *16*(1).

Marciniak, Z., Duncan, J. L., & Hu, S. J. (2002). Mechanics of sheet metal forming. In *Butterworth-Heinemann* (Vol. 16).

Martins, J. M. P., Alves, J. L., Neto, D. M., Oliveira, M. C., & Menezes, L. F. (2016). Numerical analysis of different heating systems for warm sheet metal forming. *International Journal of Advanced Manufacturing Technology*, *83*(5–8), 897–909.

Marumo, Y., Saiki, H., & Ruan, L. (2007). Effect of sheet thickness on deep drawing of metal foils. *Journal of Achievements in Materials and Manufacturing Engineering*, *20*, 479–482.

Meric, C., Koksal, N. S., & Karlik, B. (1997). An Investigation Of Deep Drawing Of Low Carbon Steel Sheets And Applications In Artificial Neural Networks. *Mathematical and Computational Applications 2*, *3,* 119–125.

Moon, Y. H., Kang, Y. K., Park, J. W., & Gong, S. R. (2001). Tool temperature control to increase the deep drawability of aluminum 1050 sheet. *International Journal of Machine Tools and Manufacture*, *41*(9), 1283–1294.

Naka, T., & Yoshida, F. (1999). Deep drawability of type 5083 aluminium-magnesium alloy sheet under various conditions of temperature and forming speed. *Journal of Materials Processing Technology*, *89–90*, 19–23.

Nguyen, V. Q., Ramamurthy, B., & Lin, J. (2014). Optimization of Influential Process Parameters on the Deep Drawing of. *Transactions of the Canadian Society for Mechanical Engineering*, *39*(3), 605–614.

Ogawa, T., Ma, N., Ueyama, M., & Harada, Y. (2016). Analysis of square cup deep-drawing test of pure titanium. *Journal of Physics: Conference Series*, *734*(3), 0–4.

Palumbo, G., Sorgente, D., Tricarico, L., Zhang, S. H., & Zheng, W. T. (2007). Numerical and experimental investigations on the effect of the heating strategy and the punch speed on the warm deep drawing of magnesium alloy AZ31. *Journal of Materials Processing Technology*, *191*(1–3), 342–346.

Pandre, S., Morchhale, A., Kotkunde, N., Singh, S. K., Khanna, N., & Saxena, A. (2021). Determination of Warm Deep Drawing Behavior of DP590 Steel Using Numerical Modeling and Experimental Process Window. *Arabian Journal for Science and Engineering*, *46*(12), 12537–12548.

Reddy, R. Venkat, Dr T.A. Janardhan Reddy, D. G. C. M. R. (2012). Effect of Various Parameters on the Wrinkling In Deep Drawing Cylindrical Cups. *International Journal of Engineering Trends and Technology*, *3*(1), 53–58.

Reddy, A. C. S., Rajesham, S., Reddy, P. R., Kumar, T. P., & Goverdhan, J. (2016). An experimental study on effect of process parameters in deep drawing using Taguchi technique. *International Journal of Engineering, Science and Technology*, *7*(1), 21.

Reddy, R. V., & Reddy, G. C. M. (2012). Effect of Various Parameters on the Wrinkling In Deep Drawing Cylindrical Cups. *International Journal of Engineering Trends and Technology*, *3*(1), 53–58.

Roy, R. K. (2001). Design of Experiments Using the Taguchi Approach: 16 Steps to Product and Process Improvement. *John Wiley & Sons, Inc*, Vol. 44, p. 560.

Saxena, R. K., & Dixit, P. M. (2009). Finite element simulation of earing defect in deep drawing. *International Journal of Advanced Manufacturing Technology*, *45*(3–4), 219–233.

Singh, C. P., & Agnihotri, G. (2015). Study of deep drawing process parameters: A review. *International Journal of Scientific and Research Publicaions*, *5*(2), 1–15.

Takuda, H., Mori, K., Masachika, T., Yamazaki, E., & Watanabe, Y. (2003). Finite element analysis of the formability of an austenitic stainless steel sheet in warm deep drawing. *Journal of Materials Processing Technology*, *143–144*(1), 242–248.

Venkateswarlu, G., Davidson, M., & Tagore, G. (2011). Influence of process parameters on the cup drawing of aluminium 7075 sheet. *International Journal of Engineering, Science and Technology*, *2*(11), 41–49.

Vrh, M., Halilovič, M., Starman, B., Štok, B., Comsa, D. S., & Banabic, D. (2014). Capability of the BBC2008 yield criterion in predicting the earing profile in cup deep drawing simulations. In *European Journal of Mechanics, A/Solids* (Vol. 45).

Zhang, K. F., Yin, D. L., & Wu, D. Z. (2006). Formability of AZ31 magnesium alloy sheets at warm working conditions. *International Journal of Machine Tools and Manufacture*, *46*(11 SPEC. ISS.), 1276–1280.

Zhang, S. H., Zhang, K., Xu, Y. C., Wang, Z. T., Xu, Y., & Wang, Z. G. (2007). Deep-drawing of magnesium alloy sheets at warm temperatures. *Journal of Materials Processing Technology*, *185*(1–3), 147–151.

PUBLICATIONS

ISI PUBLICATION: Metals, 2019

Basril, M. A. M., Azuddin, M., & Choudhury, I. A. (2019). The effect of elevated temperature on the drawability of a circular deep drawn metal cup. *Metals*, *9*(12). https://doi.org/10.3390/met9121303

CONFERENCE PAPER: International Technical Postgraduate Conference, IOP Publishing

Basril, M. A. M., Teng, H. M., Azuddin, M., & Choudhury, I. A. (2017). The effect of heating temperature and methods towards the formability of deep drawn square metal cup. *IOP Conference Series: Materials Science and Engineering*, *210*(1). https://doi.org/10.1088/1757-899X/210/1/012067

CONFERENCE PAPER: International Technical Postgraduate Conference, IOP Publishing

Basril, M. A. M., Hafsyam, Y. M., Azuddin, M., & Choudhury, I. A. (2017). The effect of elevated die temperature on deformation of deep drawn round metal cup. *IOP Conference Series: Materials Science and Engineering*, *210*(1). https://doi.org/10.1088/1757-899X/210/1/012077